Sudan University of Science and Technology

Postgraduate Collage

Multifunctional Piezoelectric System for a Mini UAV

نظام طاقة كهروضغطية متعدد المهام لطائرة مصغره من غير طيار

A Thesis Submitted to partially fulfill the Requirements for the Degree of Master of Science in Mechatronics Engineering

by:

HASSAN ABDELELAH HASSAN KOKO

Supervisor:

Dr. GIHAD ABDULAZIZ ABDULGHANI IBRAHIM

MAY 2019

الآيـــــــة

بسم الله الرحمن الرحيم

قال تعـــالي:

﴿أَوَلَمْ يَرَوْا إِلَى الطَّيْرِ فَوْقَهُمْ صَافَّاتٍ وَيَقْبِضْنَ مَا يُمْسِكُهُنَّ إِلَّا الرَّحْمَٰنُ إِنَّهُ بِكُلِّ شَيْءٍ بَصِيرٌ "﴾

" صدق الله العظيم"

سورة الملك – الآيه ﴿ 19﴾

DEDICATION

To whom I owe them every features of success that I ever had in my life. To whom strive continuously for my smile and my satisfaction, encouraged me all the way, support me under all conditions and have been the source of my strength throughout this program.

To my family

ACKNOWLEDGEMENT

Firstly, foremost all the thanks and the praise for ALLAH the most gracious the most merciful, who created this complex world in details and diversity. All the praise for ALLAH who gave me the health, the strength and the power to wind up this work.

Also, I am heartily thankful to my supervisor Dr. GIHAD IBRAHIM and my colleagues in aeronautical research and development center (ARDC) whose encouraged me, provided me valuable suggestions, recommend actions, technical information, light of guidance and other unconditional support without any expectation of personal gain during the completion of this work, I had a great honor to belong to them.

ABSTRACT

Extending the Unmanned Air Vehicles (UAV) flight time with clean energy is a new challenge. One of the pioneering technology in this filed is piezoelectric but duo to low power that can be harvested from the piezoelectric material this technology is rare. This project proposes a computational frame work to predict the maximum power that can be harvested from a piezoelectric material implanted in a UAV wing by activating the resonance mode on the piezoelectric harvester. The suitable wing selection controlled by many criteria (aspect ratio, cruse speed, physical characteristic, aerofoil shape, and availability). An equivalent wend tunnel MATLAB code was used to calculate the pressure distribution on the wing. The ANSYS structure analysis was done to b ensure that the structure has enough strength. Then the ANSYS model analysis was done to avoid resonant vibrations on wing. After that the Flutter speed was calculated then the suitable charging speed was calculated. Then the piezo - material shape, type, resonance frequency range was selected, the COMSOLE simulation for the piezoelectric material was done. The proposed frame work output was validated experimentally using a car top rig testing method. The predicted results showed good agreement to the experimental one, the output voltage reached 3.7W with power of 0.734W. Power management circuit was designed to convert the stored piezoelectric power to 5V which was then used to operate the servomotor that is used to control the UAV wing motion in comparison to previous studies that relied on iterative method, the proposed frame work output showed an improvement of (52%) which is expected to better enhance the flight endurance of UAV.

مستخلص

يمثل تمديد فترة طيران الطائرات بدون طيار بالطاقة النظيفة تحديًا جديدًا. ومن التكنولوجيات الرائدة في هذه المجال هي تكنولوجيا الطاقة الكهرضغطية ونسبة إلى الطاقة المنخفضة التي يمكن حصادها من المواد كهرضغطية تعد هذه التكنولوجيا نادرة. يقترح هذا المشروع إطار حسابي للتنبؤ بالحد الأقصى من الطاقة التي يمكن حصادها من مادة كهروضغطية مزروعه في جناح طائرة بدون طيار عن طريق تنشيط وضع الرنين على الحصادة الكهرضغطية. اختيار الجناح المناسب يتم التحكم فيه بواسطة العديد من المعايير (نسبة العرض إلى الطول ، سرعة الطيران ، الخصائص الفيزيائية ، شكل الطيران ، وامكانية التصنيع). تم استخدام كود ماتلاب مكافئ للنفق الهوائي لحساب توزيع الضغط على الجناح. تم إجراء تحليل لهيكل الجناح للتأكد من أن الهيكل لديه قوة كافية لتحمل الضغوط المسلطة عليه .ومن ثم تم إجراء التحليل النموذجي لحساب الاهتزازات الرنانة على الجناح. بعد ذلك تم حساب سرعة الرفرفة ثم تم حساب سرعة الشحن المناسبة. وبعد ذلك تم اختيار (شكل المادة الكهروضغطيه - نوعها - ونطاق تردد الرنين الخاص بها) وبعد ذبك تم إجراء محاكاة ببرنامج حاسوبي لخصائص المادة الكهرضغطية. تم التحقق من صحة إطار العمل المقترح بشكل تجريبي باستخدام طريقة اختبار المنصة المثبتة اعلي السيارة . أظهرت النتائج المتوقعة توافقًا جيدًا مع النتائج التجريبية ، حيث وصل جهد الخرج الي 3.7 فولت بقدرة كهربائية 0.734 واط وايضا تم تصميم دائرة كهربيه لتحويل الخرج الي 5 فولت ومن ثم استخدمت الطاقة الكهروإجهادية المخزنة لتشغيل الموتور الذي يستخدم للتحكم في حركة جناح الطائرة بدون طيار. مقارنة بالدراسات السابقة التي اعتمدت على الطريقة التكرارية ادت طريقة العمل المقترحة لتحسين الاداء لنظام حصاد الطاقة بنسبة (52%) .هذا التحسين في الاداء يظهر بصورة واضحه كذياده في مدة طيران الطائرة بدون طيار.

TABLE OF CONTENTS

LIST OF TABLES

LIST OF FIGURES

LIST OF ABBREVIATIONS

DC	Direct Current
UAV	Un Manned Air Vehicle
Km	Kilometer
AC	Alternative Current
PVDF	polymer
MFC	Micro-Fiber Composites
ZnO	Zinc-Oxide
MPPT	Maximum Power Point Tracker
M1U	Half-Wave Rectification
B2U	Full-Wave Rectification
SMPS	Switched-Mode Power Supply
ALUs	Arithmetic Logic Units
FETs	Field-Effect Transistors
MOSFETs	Metal–Oxide–Semiconductor Field-Effect Transistors
AOI	And-Or-Invert
OAI	Or-And-Invert
Li	Lithium Ion
RC	Radio-Controlled
EP	Electric Power
AR	Aspect Ratio
PZT	Zirconate Titanate
SHM	Structural Health Monitoring
AOA	Angle of Attack
LED	Light Emitted Diode

LIST OF SYMBOLS

C_{pq}^{E}	Young's module
e_{KP}	piezoelectric coefficient
ζ_{ik}^{S}	clamped permittivity.
Jp	current density is
d xx	the Mode of Generators
g yy	generated voltage
a(t)	acceleration of the vibration
L	Beam length
b	Beam width
hp	Piezoelectric layer thickness
hs	Substrate layer thickness
lm	End mass length
lb	End mass width
lh	End mass thickness
Ys	Young's modulus of substrate material
Yp	Young's modulus of piezoelectric material
ρs	Mass density of piezoelectric material
ρp	Mass density of substrate material
ρm	Mass density of end mass material
R	Load resistance
D	duty cycle
di	ripple current
L	inductor value
dv	voltage ripple
T	Stress
S	Strain
E	Electric Field
D	Electrical Induction

M	Mass
b	Damping Coefficient
k	Stiffness
C	Capacitor
M	Meter
W	Watt
Ft	Feet

1 CHAPTER ONE

INTRODUCTION

1.1 Motivation

Renewable energy sources are becoming the future of our electricity. It is cheap efficient and does not have negative effect on the environment. (Ambient Energy harvesting is the process of converting available ambient energy into usable electrical energy using a particular material or transduction mechanism) Anton [1]. Several classes of material exist with various conversion mechanisms that can be used to harvest energy. Some of the common materials include those with photovoltaic coupling to convert solar energy to electric energy, thermoelectric coupling to convert temperature gradients into electrical energy, and electromechanical coupling to convert mechanical vibration energy into electrical energy. For Small-scale solar it is moderately small and medium cost but Low power generation indoors e.g. Sol Chip and Panasonic are 5 and 60mW DC with indoor lighting, respectively. For the Thermal energy generators, they are large and high cost, Non-standard materials and requires large cooling fins and heat sinks. Actually, the vibration energy harvesting is the most versatile technique being developed in the literature. Three main mechanisms of vibration-to-electrical energy conversion exist including electrostatic, electromagnetic, and piezoelectric transduction. By reviewing work performed on all of the transduction mechanisms of the three modes of vibration harvesting, piezoelectric energy harvesting has received the most attention.

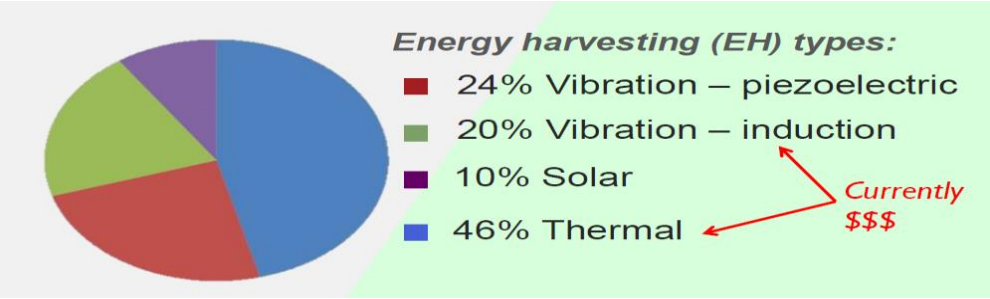

Figure 1-1 energy harvesting types IDTechEx [2]

Its generates energy from weight, motion, vibration and temperature changes. The harvested energy can be stored in a battery to be used in a useful purpose. On the other hand, the piezoelectric material has the ability to make movement when it was effected by electrical signal Piezoelectric vibration harvesting is attractive mainly due to the simplicity of piezoelectric transduction and the relative ease of implementation of piezoelectric systems into a wide variety of applications as compared to electrostatic or electromagnetic methods e.g. It can be configured to generate and store energy from roads, airport runways, railway systems and air flow over the surface of the flaying vehicles etc. unlike electrostatic transduction, which requires the application of an initial voltage to produce usable energy, piezoelectric material inherently generates a direct voltage when strained. Additionally, where electromagnetic harvesting systems become increasingly difficult to fabricate at the micro-scale and electrostatic systems are generally restricted to the micro-scale, piezoelectric materials can easily be fabricated as bulk materials at the macro scale or deposited as thin-films at the micro-scale. Despite these advantages, piezoelectric harvesting does suffer from the large mass density of piezo ceramic materials and, like all vibration harvesting techniques, the intrusiveness that an added harvesting system has on a host structure (i.e. the vibration harvesters gain its vibration from the structure that it is attached to). In an effort to increase the usefulness of various material systems, researchers have begun to investigate the concept of multifunctionality, a multifunctional approach means combining several functions into a single device, such as energy harvesting, energy Storage, and structural load bearing ability, that when combined with a host structure can provide a more synergistic and efficient overall system. And it is also a type of multi-functionality when the two phenomena of the piezo is used at the same system to prove electrical energy and mechanical energy the introduction of multi-functionality into energy harvesting systems holds promise to increase their utility and practicality, and promote the integration of harvesting systems into many engineering applications. Usually the power harvested from the vibration generated by the aerodynamic forces is

calculated by mili-watts and microwatts so it is suitable for the low power electronics. The energy requirements of low-power electronics have steadily decreased with advancements in efficient circuitry such that energy harvesting systems can be considered feasible solutions in providing power to self-powered systems. Conventional low-power electronics, such as wireless sensor nodes, rely on batteries to provide power to the device. The use of batteries, however, presents several drawbacks including the cost of battery replacement as well as limitations imposed by the need of convenient access to the device for battery replacement purposes. Wireless sensor nodes, for example, are often used in remote locations or embedded into a structure; therefore, access to the device can be difficult or impossible. By scavenging ambient energy surrounding an electronic device, energy-harvesting solutions have the ability to provide permanent power sources that do not require periodic replacement. Such systems can operate in an autonomous, self-powered manner, reducing the costs associated with battery replacement, and can easily be placed in remote locations or embedded into host structures.

1.2 Problem Statement

Extending the Unmanned Air Vehicles (UAV) flight time with clean energy is a new challenge. One of the pioneering technology in this filed is piezoelectric but duo to low power that can be harvested from the piezoelectric material this technology is rare

1.3 Objectives

The main objective of this thesis are:

- Suitable Wing selection based on (physical characteristic, AR, cruse speed and airfoil shape)
- Apply the vibration analyses to the selected wing to predict the resonance frequency
- Calculating the optimum charging speed, the UAV and Select a suitable power harvester

- finite element analyses of the selected harvester to estimate the output voltage
- Design the power management circuit using MATLAB software to convert the harvester output to the required voltage output
- experimental implementation of the developed methodology and system

1.4 methodology

The wigs selection is the first step it controlled by many criteria (aspect ratio , cruse speed ,physical characteristic ,air foil shape ,and availability).The aspect ratio of a wing is the ratio of its span to its mean chord In the field of piezoelectric power generation the best wing type is that one have the highest aspect ratio to its flexibility and to get the highest wing flexibility it better to fly near to the flutter speed and that is also can be applied by the high AR wings on very low velocity. The cruse speed is a speed on the flight phase. It depends on the type of wind but usually on the highest speeds the harvested power will be more than the lower so it's better to select airfoils that con fly at high speeds. Wing physical characteristic: this criterion can't be neglected at all. the wings dimensions and weights is related to the above and also effect on the flutter and the natural frequency(Natural frequency is the frequency at which a system tends to oscillate in the absence of any driving or damping force.) for the safety of aircraft the frequencies of each velocity must be determined to avoid the matching between the vibration generated by aerodynamic forces and the natural frequency on the wing it self .the result on the matching will generate a huge damage on the structure . Based on the above criteria the selected wing will tested in Wind tunnel equivalent model to calculate Pressure distribution on the wing.

1.5 Thesis layout

This thesis consists of five chapters. chapter one includes motivation, problem statement, objective and methodology. Chapter two will be on the part of concepts and theory of the pizoelectrical phenomena, electromechanical modeling of the pizoelectrical generator and power control circuit also the previous studies will be discussed in details. Chapter three will be on the system

design including selected wing vibration analyses by developed wind tunnel equivalent model to analyze the impact of the airflow on the surface of the wing that will make it easy to predict the amount of frequency range that is suitable for the piezoelectric generator to work on effective way then testing software equivalent model for the piezoelectric harvester and power management simulation .Chapter four is the experimental part start from piezoelectric generator selection then the implementation of the control system and power conditioning circuit after that the car top rig test . Finally showing the results of the experiments and make Discussions about it. Chapter five the last chapter contents the conclusion and the recommendation for the further work

2 CHAPTER TWO

BACKGROUND AND LITERATURE REVIEW

2.1 Piezoelectric Energy Harvesting

Figure 2-1 shows the hierarchy of main energy harvesting technologies

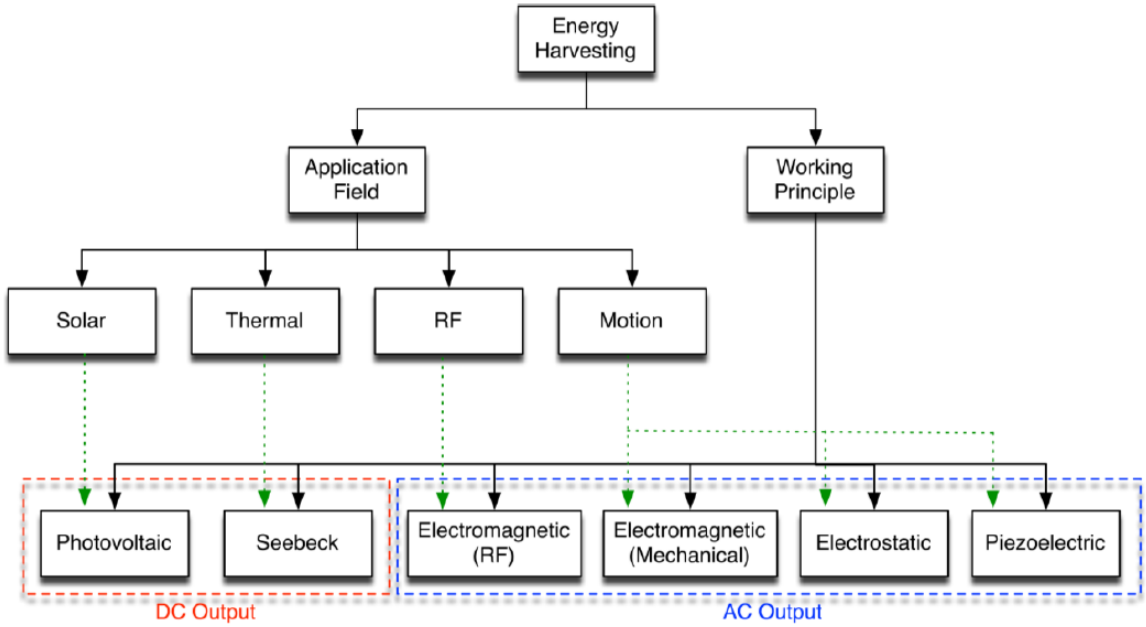

Figure 2-1 Hierarchy of main energy harvesting technologies.

The possibility and the effectiveness of extracting energy from human activities has been under study for years as a matter of fact, continuous and uninterrupted power can potentially be available: from typing (1mW), motion of upper limbs (10mW), air exhalation while breathing (100mW), walking (1W)as shown in Figure 2-2. Among available motion based harvesting techniques, piezoelectric transduction offers higher power densities in comparison to electrostatic transduction (which also needs an initial polarization). Also, piezoelectric technologies are better suited than electromagnetic ones for micro electromechanically systems (MEMS) implementation, because of the limitations in magnets miniaturization with current state-of-the-art micro fabrication processes

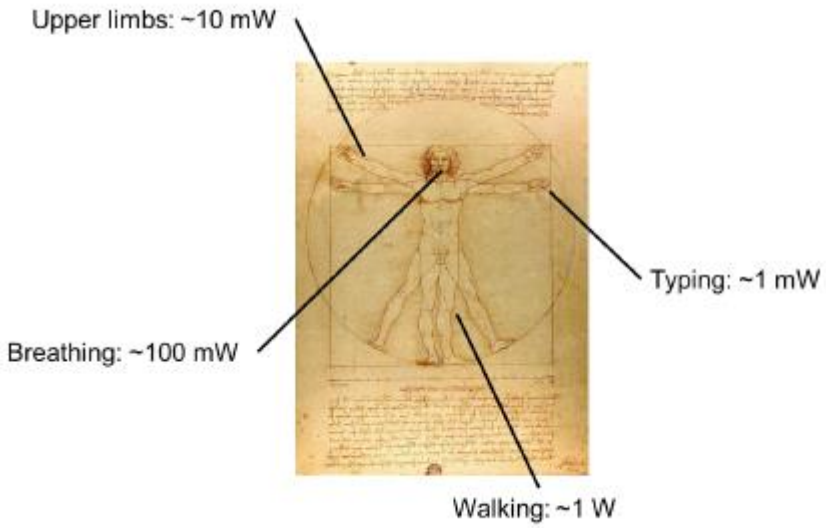

Figure 2-2 energy from human activities

The piezoelectric effect converts mechanical strain into electric current or voltage. It is based on the fundamental structure of a crystal lattice. Certain crystalline structures have a charge balance with negative and positive polarization, which neutralize along the imaginary polar axis. When this charge balance is perturbed with external stress onto the crystal mesh, the energy is transferred by electric charge carriers creating a current in the crystal. Conversely, with the piezoelectric effect an external charge input will create an unbalance in the neutral charge state causing mechanical stress. The connection between piezoelectricity and crystal symmetry are closely established. The piezoelectric effect is observed in crystals without center of symmetry, and the relationship can be explained with monocrystal and polycrystalline structures.

In a monocrystal Figure 2-3 the polar axes of all of the charge carriers exhibit one-way directional characteristics. These crystals demonstrate symmetry, where the polar axes throughout the crystal would lie unidirectional even if it was split into pieces.

Figure 2-3 monocrystal

Instead, a polycrystal as shows in Figure 2-4 is characterized by different regions within the material with different polar axes. It is asymmetrical because there is no point at which the crystal could be cut that would leave the two remaining pieces with the same resultant polar axes.

In order to attain the piezoelectric effect, the polycrystal is heated to the Curie point along with strong electric field. The heat allows the molecules to move more freely and the electric field forces the dipoles to rearrange in accordance with the external field as shown in Figure 2-5.

Figure 2-4 polycrystal

Figure 2-5 electrical force effect

As a result, the material possesses piezoelectric effect: a voltage of the same polarity as of the poling voltage appears between electrodes when the material is compressed; and opposite polarity appears when stretched. Material deformation takes place when a voltage difference is applied, and if an AC signal is applied the material will vibrate at the same frequency as the signal.

Piezoelectricity is governed by the following constitutive equations, which link the stress T, the strain S, the electric field E and the electrical induction D

$$T_p = C_{pq}^{E} S_q - e_{KP} E_k \tag{2-1}$$

$$D_i = e_{iq} S_q + \zeta_{ik}^{S} E_k \tag{2-2}$$

Where:

ζ_{ik}^{S} piezoelectric coefficient, e_{KP} Young's modulus, C_{pq}^{E} clamped permittivity.

Figure 2-6 shows the Schematic representation of the concept of a piezoelectric energy harvesting system

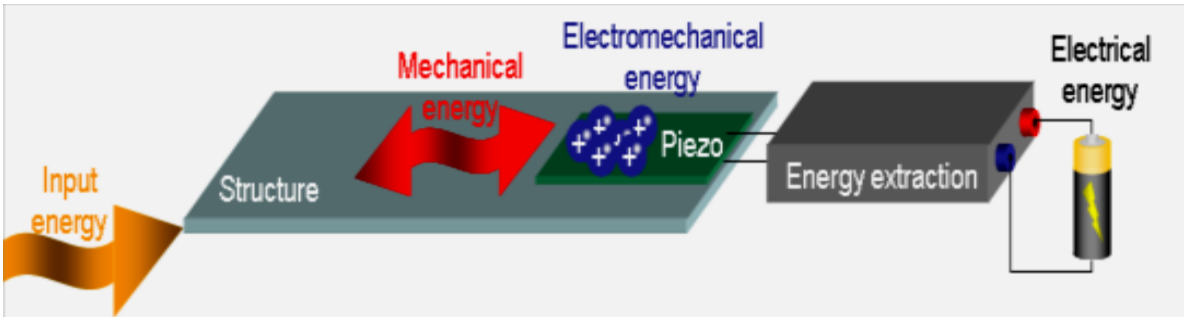

Figure 2-6 Schematic representation of the concept of a piezoelectric energy harvesting system

2.2 Vibration source

First, the process is to study the vibration source that the energy harvester will harvest Power from it. the following tables will show some

Table 2-1 vibration sources

	Highest Power Peak (HPP)		Reference Peak (RP)		Alternate Peak (AP)	
Source	Acc [m/s^2]	Freq [Hz]	Acc [m/s^2]	Freq [Hz]	Acc [m/s^2]	Freq [Hz]
A/C duct center (Low setting)	0.0328	15.7	0.0254	171.9	0.0130	113.8
A/C duct side (High setting)	0.0990	53.8	0.0159	170.6	0.0127	~100
A/C duct center (Low setting)	0.0398	55.0	0.0366	173.1	0.0186	108.3
Computer side panel	0.0402	276.3	0.0402	276.3	0.0360	120.0
Microwave oven top	1.11	120.0	1.11	120.0	0.570	240.0
Microwave oven side	4.21	148.1	4.21	148.1	1.276	120.0
Office desk	0.0879	120.0	0.0879	120.0	0.00516	546.3
Bridge railing	0.0215	171.3	0.0215	171.3	0.0193	136.3
Parking meter (Perpendicular to street)	0.0327	13.8	0.00172	120.0	0.000697	148.1
Parking meter (Parallel to street)	0.0355	13.8	0.00207	923.8	0.000509	977.5
Car hood—750 rpm	0.0744	35.6	0.0143	148.8	0.0103	510.6
Car hood—3000 rpm	0.257	147.5	0.257	147.5	0.102	880.6
Medium tree	0.000985	16.3	0.000229	115.3	0.000226	240.0
Small tree	0.003	30.0	0.000465	293.1	0.000425	99.4

2.3 Materials

Each piezoelectric material can be characterized with a set of parameters. For example, relationship between the applied stress and the electric induction D (therefore, current density is $j_p = \frac{dD}{dt}$).The mechanical characteristics (Young's modulus) define the robustness and toughness of the device and also play an important role in defining piezoelectric coefficients. Dielectric permittivity also plays a similar role in definitions. All these parameters (determined by the material) are crucial in designing a harvesting system, making in turn material selection a primary factor in piezoelectric harvesters. Table 2-2 lists some of the most common piezoelectric materials, mainly piezo ceramics (that are polarized ferroelectric ceramics), such as piezo Zirconate Titanate (PZT) and barium titanate. Out of them, PVDF polymer and Micro-Fiber Composites (MFC) as highly flexible materials. MFCs are composites that combine the energy density of piezoceramic materials with the flexibility of epoxy. The researchers compared PZT with PVDF and MFC, they showed that although PZT shows the highest power density, it is not well suited for high g-vibrations because of its lower yield strength that results in lower robustness, leading to fracture. Furthermore, zinc-oxide (ZnO) is an interesting material that is pushing the piezoelectric field to a nanometric scale. It is used to grow one dimensional hair-like nanowires, with diameters in the sub-one hundred nanometer scale and lengths ranging from several hundreds of nanometers to a few centimeters. Zinc exhibits both semiconductor and piezoelectric properties, it is relatively biosafe and biocompatible, so it can be involved in biomedical applications with little toxicity The piezoelectric properties change logarithmically with age allowing them to stabilize. Therefore, manufacturers usually specify the constants of the material after a period of time

Table 2-2 Coefficients for common piezoelectric materials

Compound	d_{33}	d_{31}	d_{15}	g_{33}	g_{31}	g_{15}	Curie Point [°C]
	$[10^{-12}$ C N$^{-1}]$			$[10^{-3}$ V m N$^{-1}]$			
PZT-2	152	−60.2	440	38.1	−15.1	50.3	370
PZT-4	289	−123	496	26.1	−11.1	39.4	328
PZT-5A	374	−171	584	24.8	−11.4	38.2	365
PZT-5H	593	−274	741	19.7	−9.1	26.8	193
PZT-8	225	−37	330	25.4	−10.9	28.9	300
Pz21	640	−259	616	15.6	−7.4	26.8	218
Pz23	328	−128	421	24.7	−9.6	34.3	350
Pz24	149	−58	247	39.7	−15.4	37.7	330
Pz26	328	−128	327	28	−10.9	38.9	330
Pz27	425	−170	506	26.7	−10.7	37.3	350
Pz28	275	−114	403	31.4	−13	37.3	330
Pz29	574	−243	724	22.6	−9.6	32.1	235
Pz34	46	−5.33	43.3	25	−2.9	27.9	400
Ceramic B	149	−58	242	14.1	−5.5	21	115
$BaTiO_3$	145	−58	245	13.1	−5.2	20.5	120
PVDF	−33	23	-	330	216	-	100
0.70PMN-0.30PT	1,611	−2,517	157	29.2	−45.6	9	150
0.69PMN-0.31PT	-	-	5,980	-	-	56	146
MFC M8528	460	−210	-	-	-	-	80

Where

- d_{xx} is the Mode of generators
- g_{yy} is the generated voltage

2.4 Resonant Devices

The main types of this generators are:

2.4.1 D 31 Mode Generators

In operating mode, the material has an induced electric field in direction 3, as a response to the stress along direction 1. Figure 2-7 shows the most common configuration of a piezoelectric harvester, which comprises of a rectangular beam, a tip mass and a piezoelectric material.

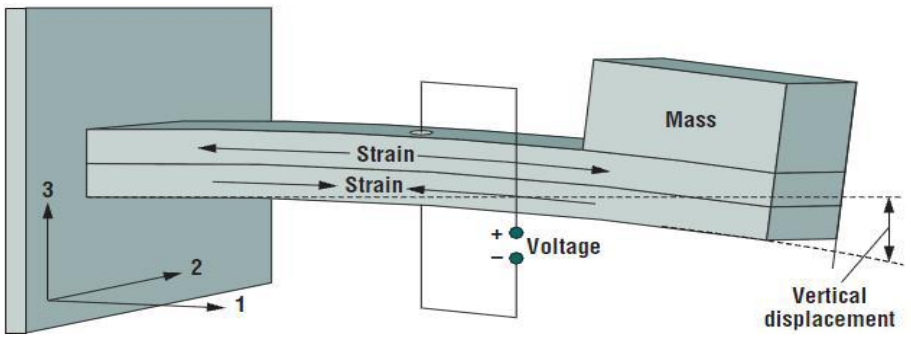

Figure 2-7 Rectangular cantilever beam

2.4.2 D 33 mode generators

In D33 operating mode the material is subjected to a stress in the same direction of the produced electric field. This operating mode led initially to impact harvesters while vibrating generators were made only via D31effect. However, several researchers focused on fabricating vibrating devices with alternative modes to. There is a fact that piezoelectric coefficients in D33and D15 modes are higher than ones Table 2-3 so this can possibly lead to devices with higher output power. D33 Vibrating generators can be used. For example, in industrial fields such as automotive and machinery or wherever there are mechanical joints that, due to tolerances, show relative movements between structural components. The cyclical movement of structures, due for example to the effect induced by the vibrational dynamics of the system, can be exploited by adopting appropriate mechatronic systems. Their geometry and their structure is able to convert macroscopic displacement (in the order of millimeters) into a high force microscopic motion acceptable by the piezoelectric material.

Table 2-3 Resonant devices comparison.

Reference	Material		d_{ij}	V_{device}	V_{piezo}	f_n	R_L	V_{OUT}	$P_{density}$	Power Factor
	Name	Mode	[pm/V]	[mm^3]	[mm^3]	[Hz]	[Ω]	[V]	[W/cm^3]	[$W/(g^2cm^3)$]
[78]	AlN	d_{31}	-	0.5	0.0004	1.4×10^3	650×10^3	1.6	4×10^{-3}	248×10^{-6}
[48]	PZT	d_{31}	320	212.5	80.4	223.8	9.9×10^3	-	77×10^{-6}	1.4×10^{-6}
[61]	PZT	d_{33}	-	-	0.00002	13.9×10^3	5.2×10^6	2.4 dc	-	-
[63]	PZT	d_{33}	100	3.5	0.014	118.1	4.5×10^6	4.7	136×10^{-6}	543×10^{-6}
	PZT	d_{31}	−55	3.5	0.014	130.8	11×10^3	0.77	1.9×10^{-3}	7.8×10^{-3}
[57]	PZT	d_{33}	100	1.1	0.003	243	2×10^6	2 rms	1.6×10^{-3}	6.4×10^{-3}
	PZT	d_{31}	−55	1.1	0.003	243	9.9×10^3	1.5 rms	2×10^{-3}	8.1×10^{-3}
[77]	PZT	d_{15}	700	171.2	65	73	2.2×10^6	6.2	51×10^{-6}	-
[76]	PZT	d_{15}	741	4.8	2.5	45	1.6×10^6	19×10^{-3} rms	87×10^{-6}	67.8×10^{-3}
[74]	PMN-PT	d_{15}	3,080	24,100	156	-	91×10^3	11.3	29×10^{-6}	189×10^{-9}
[35]	ZnO	d_{31}	10	-	9.7	10×10^6	500×10^6	8×10^{-3}	4×10^{-6}	624×10^{-15}
[68]	MFC	d_{33}	400	340	120	22.5	4×10^6	-	494×10^{-6}	17.1×10^{-3}
[69]	PVDF	d_{33}	33	549.5	24.2	1.5	10×10^6	-	364×10^{-6}	-

The last column reports the power factor, i.e., the output power density normalized with the input acceleration Based on the analysis of various configurations in the reviewed literature, we can point out that D31 represents the most used operating mode for piezoelectric-based devices. As an example, a

possible application of D33 generators is represented by the car door latch system shown in Figure 2-9.

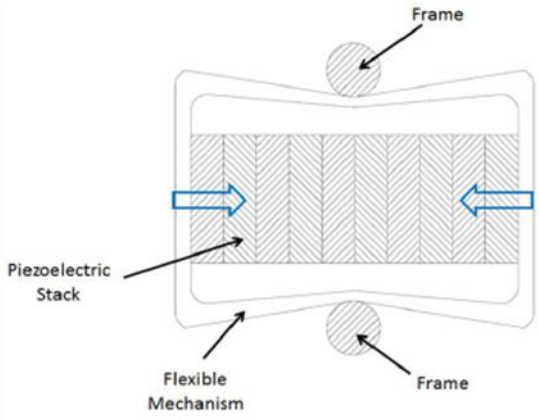

Figure 2-9 possible architecture of the harvester.

This assembly shows a cyclic displacement (highest value ~1mm) with frequency range between 0 and 10Hz. In this view, it is possible to design an electromechanical system with a metal frame, to be coupled with the internal part of the closure, able to scale the displacement in values compatible with piezo stacks as shown at Figure 2-8.

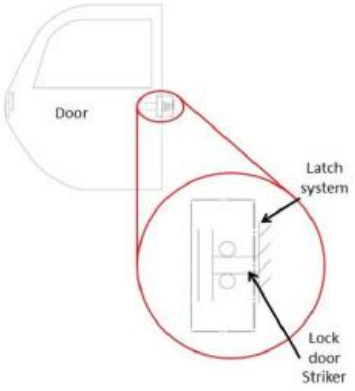

Figure 2-8 Car door latch system

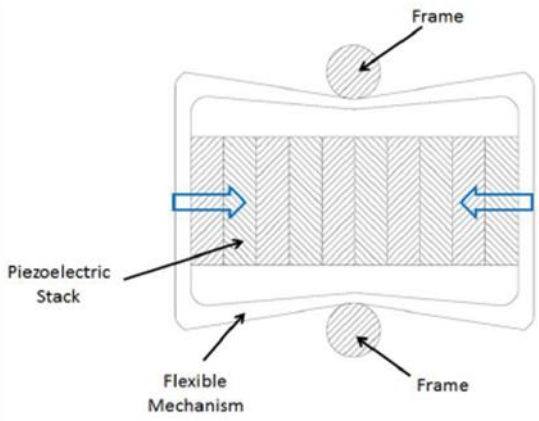

Figure 2-9 possible architecture of the harvester.

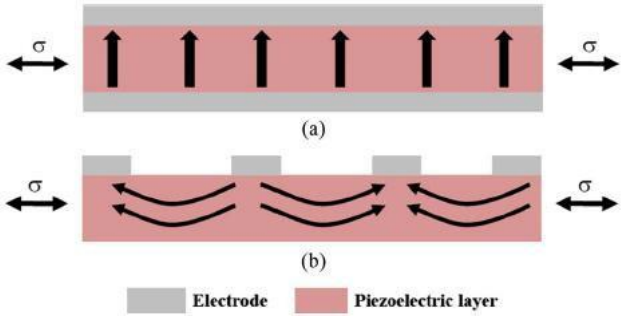

Figure 2-10 Polarization with D31 mode (a) and D33 mode (b) piezoelectric harvesters

2.4.3 D15 mode generators

D15 Operating mode characterizes shear stress harvesters. In this mode the piezoelectric material is polarized along direction 1 and is subjected to a shear stress σ_{31}. The electrical output is perpendicular to both the polarization and the applied stress. The main problem of these devices is related to the perpendicularity of the polarization direction and the electrical output Figure 2-11 which constrains to use a set of electrodes for the polarization and a different set of electrodes for operation.

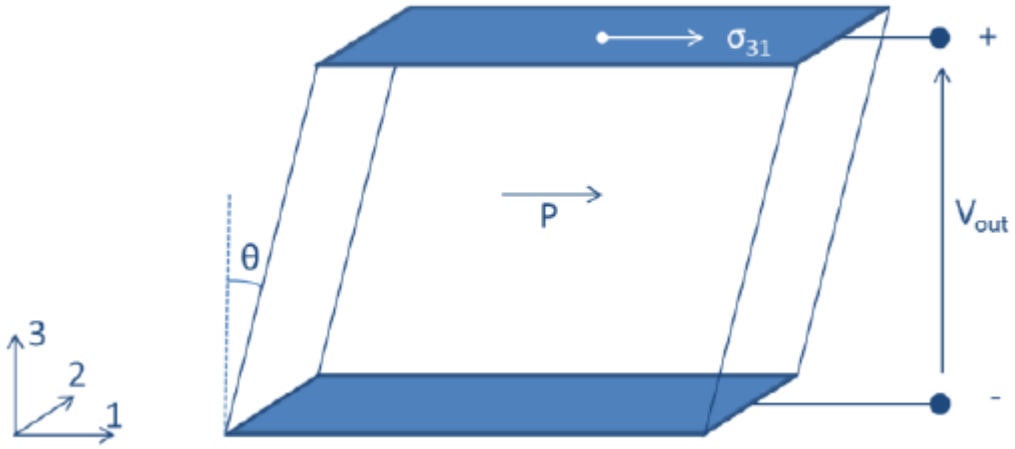

Figure 2-11 Shear stress harvester (operating mode)

2.5 Optimal Shapes

Rectangular cantilever beams often suffer from over strain at the long length, but when the shape is tending to trapezoidal it is more strong and able to prevent the material from the over strain, as shown in Figure 2-12 the maximum allowable strain is higher in the trapezoidal shape

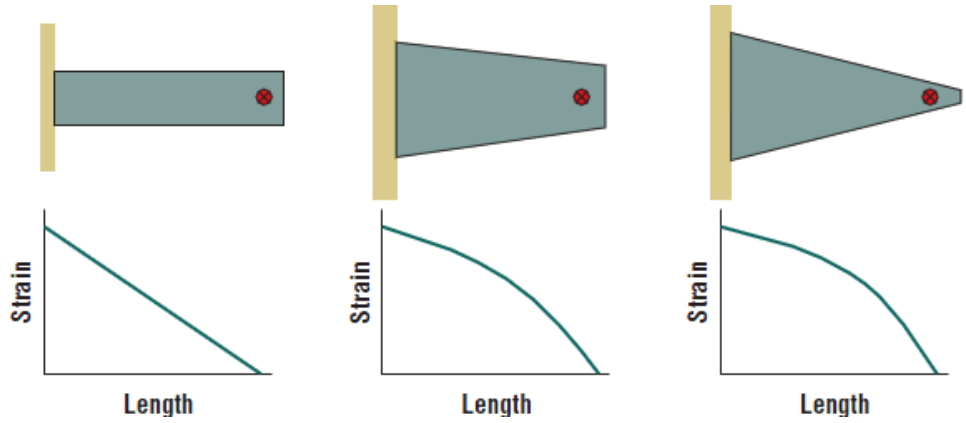

Figure 2-12 Trapezoidal beams [99]

2.6 Frequency Tuning

To provide optimal power output the harvester resonant frequency must matches the dominate frequency of the system it is harvesting energy from. Most piezoelectric harvesters can be tuned to a wide range of frequencies. By adding tip mass greatly reduces the resonant frequency and by changing the location of the harvester in the test area. One of the effective elements is the acceleration

amplitudes the following figure shows the effect of acceleration on the output power at the 6hz for acceleration amplitudes (0.25g,0,5g,1g, and 2g)

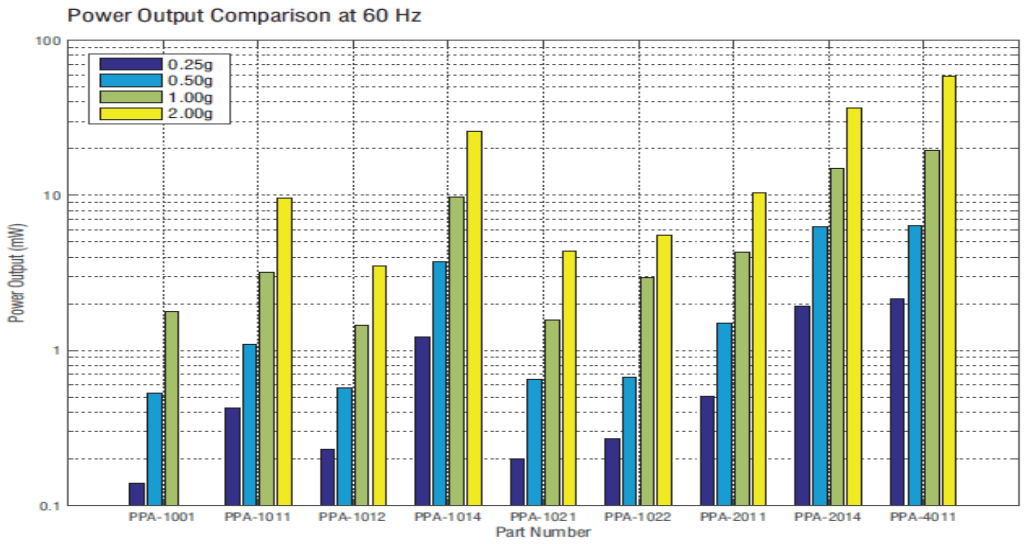

Figure 2-13 the power output of each product when tuned to 60 Hz for four different acceleration amplitudes

The next comparison is for the effect of the tip mass on the output power for the piezo protection advantage (PPA) products The tip mass weight is just 0.5g but the effect on the output power is very clear as shown in Figure 2-14

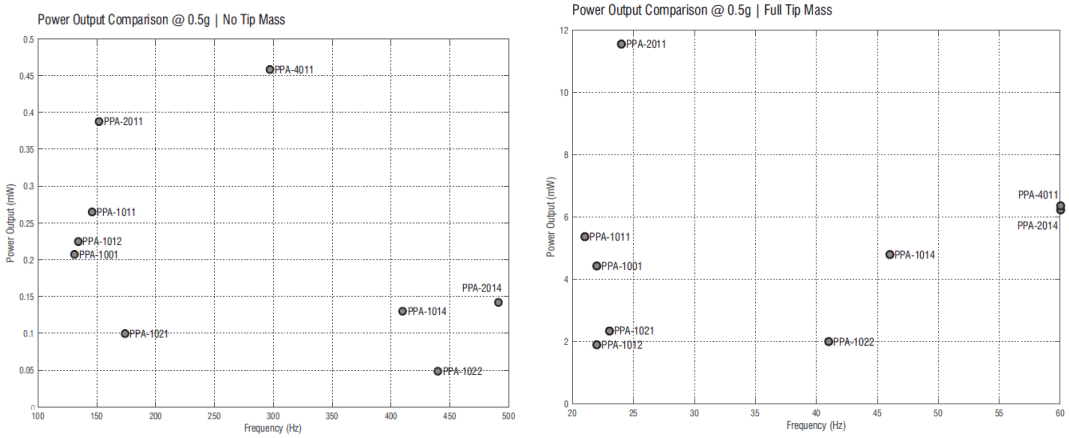

Figure 2-14 tip mass effect

2.7 Non-resonant devices

On this type of devices there is no vibration source the vibration is self-generated by internal mechanism. For example, the design of this device shown in Figure 2-15 derives from the inverted pendulum; in which reaction forces from two permanent magnets are used (one on the tip mass of cantilever, and the other just in front on an adjustable stage) to provide two stable states.

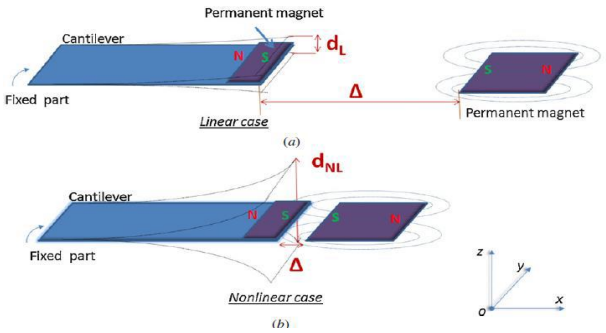

Figure 2-15 non-resonant devices using permanent magnet

2.8 Rotational Devices

The idea of those devices is mainly by transforming a rotatory excitation into a longitudinal strain. Among these, Gu and Livermore presented a compact self-tuning rotatory harvester, consisting in a rigid piezoelectric beam and a flexible beam with a tip mass at its end (a steel ball). During operation, the steel ball impacts the generating beam, letting it to vibrate. The system natural frequency is determined by the flexible beam natural frequency, which varies with the imposed centrifugal force. KHAMENEIFAR and colleagues applied the piezoelectric cantilever concept to a rotating shaft as shown in Figure 2-16. This approach allows employing a piezoelectric device for monitoring rotating machines such as turbines or tires. The device (employing a single PZT element with a single 5 cm length cantilever beam and a 105g tip mass) driven at 138 rad/s was able to harvest 6.4mW on an optimum load resistance of 40kΩ, with a corresponding output voltage of about 16V.

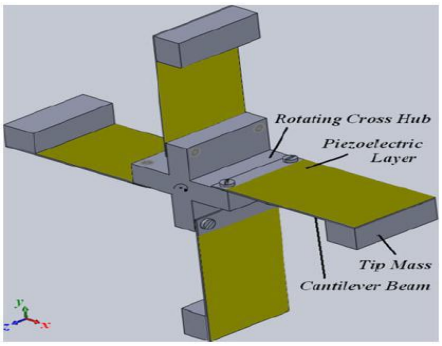

Figure 2-16 Rotary devices concept

2.9 Power Conditioning Circuit Elements

Figure 2-17 Shows the power conditioning circuit elements

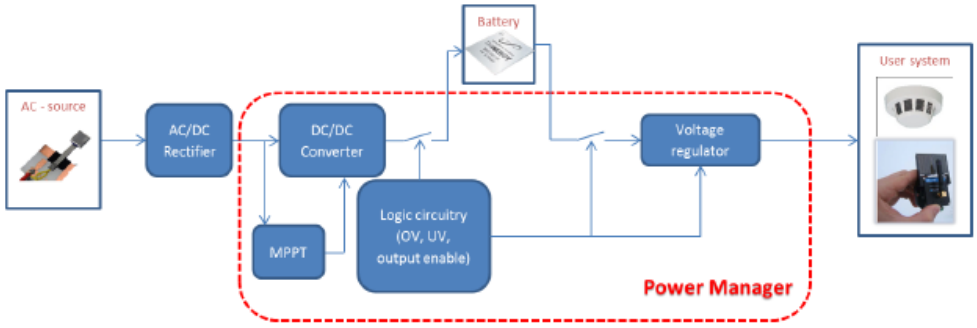

Figure 2-17 Power conditioning circuit elements

Power managers are designed both for direct current (DC) and AC sources. They typically employ a DC-DC converter, mainly for impedance matching and also to match the source voltage with the battery charging level. In case of alternate sources, a rectifier is required. In case of direct current sources, impedance matching can be achieved through the use of a Maximum Power Point Tracker (MPPT). It implements algorithms apt (arbitrary sub-population tracker) to follow the input power peaks, which is equivalent to fix the generator operating point by acting on the equivalent impedance of the downstream circuitry. The logic circuitry is designated to control and manage the charge and discharge phases of the battery. Overvoltage and under voltage boundaries can be controlled with the help of comparators and switches. Voltage thresholds are often configurable by users using resistive dividers. Piezoelectric generators are AC sources, hence their output has to be rectified and regulated to supply host devices. The main power conditioning elements are:

2.9.1 Rectifier

A rectifier is an electrical device that converts AC, which periodically reverses direction, to DC, which flows in only one direction. The process is known as rectification, since it "straightens" the direction of current. Physically, rectifiers take a number of forms, including vacuum tube diodes, mercury-arc valves, copper and selenium oxide rectifiers, semiconductor diodes, silicon-controlled rectifiers and other silicon-based semiconductor switches. Historically,

even synchronous electromechanical switches and motors have been used. Early radio receivers, called crystal radios, used a "cat's whisker" of fine wire pressing on a crystal of galena (lead sulfide) to serve as a point-contact rectifier or "crystal detector".

2.9.2 DC-to-DC converter

A DC-to-DC converter is an electronic circuit or electromechanical device that converts a source of DC from one voltage level to another. It is a type of electric power converter. Power levels range from very low (small batteries) to very high (high-voltage power transmission).

- **Step-down:** A converter where output voltage is lower than the input voltage such as a buck converter.

For the circuit of the multi-functional system the output of the harvester will be at small value so the step up boost converter will be used

- **A boost converter** (step-up converter) is a DC-to-DC power converter that steps up voltage (while stepping down current) from its input (supply) to its output (load). It is a class of Switched-Mode Power Supply (SMPS) containing at least two semiconductors (a diode and a transistor) and at least one energy storage element: a capacitor, inductor, or the two in combination. To reduce voltage ripple, filters made of capacitors (sometimes in combination with inductors) are normally added to such a converter's output (load-side filter) and input (supply-side filter).shows the schematic of the boost converter

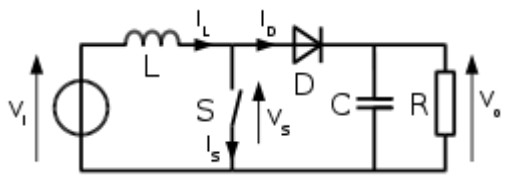

Figure 2-18 Boost converter schematic

2.9.3 Maximum Power Point Tracking

MPPT is algorithm that included in charge controllers used for extracting maximum available power from PV module under certain conditions. The voltage at which power voltage (PV) module can produce maximum power is called ‘maximum power point’ (or peak power voltage). Maximum power varies with

vibration frequency, amplitude and harvester type. The major principle of MPPT is to extract the maximum available power from harvester module by making them operate at the most efficient voltage (maximum power point). That is to say: MPPT checks output of harvester module, compares it to battery voltage then fixes what is the best power that harvester module can produce to charge the battery and converts it to the best voltage to get maximum current into battery. It can also supply power to a DC load, which is connected directly to the battery.

2.9.4 Logic circuit

In electronics, a logic gate is an idealized or physical device implementing a Boolean function; that is, it performs a logical operation on one or more binary inputs and produces a single binary output. Depending on the context, the term may refer to an ideal logic gate, one that has for instance zero rise time and unlimited fan-out, or it may refer to a non-ideal physical device Logic gates are primarily implemented using diodes or transistors acting as electronic switches, but can also be constructed using vacuum tubes, electromagnetic relays (relay logic), fluidic logic, pneumatic logic, optics, molecules, or even mechanical elements. With amplification, logic gates can be cascaded in the same way that Boolean functions can be composed, allowing the construction of a physical model of all of Boolean logic, and therefore, all of the algorithms and mathematics that can be described with Boolean logic. Logic circuits include such devices as multiplexers, registers, arithmetic logic units (ALUs), and computer memory, all the way up through complete microprocessors, which may contain more than 100 million gates. In modern practice, most gates are made from field-effect transistors (FETs), particularly metal oxide semiconductor Field-Effect Transistors (MOSFETs). Compound logic gates AND-OR-Invert (AOI) and OR-AND-Invert (OAI) are often employed in circuit design because their construction using MOSFETs is simpler and more efficient than the sum of the individual gates.

2.9.5 Voltage regulator

A voltage regulator is designed to automatically maintain a constant voltage level. A voltage regulator may be a simple feed-forward design or may include negative feedback. It may use an electromechanical mechanism, or electronic components. Depending on the design, it may be used to regulate one or more AC or DC voltages. Electronic voltage regulators are found in devices such as computer power supplies where they stabilize the DC voltages used by the processor and other elements. In automobile alternators and central power station generator plants, voltage regulators control the output of the plant. In an electric power distribution system, voltage regulators may be installed at a substation or along distribution lines so that all customers receive steady voltage independent of how much power is drawn from the line

2.9.6 Battery

An electric battery is a device consisting of one or more electrochemical cells with external connections provided to power electrical devices such as flashlights, smartphones, and cars. When a battery is supplying electric power, its positive terminal is the cathode and its negative terminal is the anode. The terminal marked negative is the source of electrons that when connected to an external circuit will flow and deliver energy to an external device. When a battery is connected to an external circuit, electrolytes are able to move as ions within, allowing the chemical reactions to be completed at the separate terminals and so deliver energy to the external circuit. It is the movement of those ions within the battery which allows current to flow out of the battery to perform work. Historically the term "battery" specifically referred to a device composed of multiple cells, however the usage has evolved additionally to include devices composed of a single cell. Primary (single-use or "disposable") batteries are used once and discarded; the electrode materials are irreversibly changed during discharge. Common examples are the alkaline battery used for flashlights and a multitude of portable electronic devices. Secondary (rechargeable) batteries can

be discharged and recharged multiple times using an applied electric current; the original composition of the electrodes can be restored by reverse current. Examples include the lead-acid batteries used in vehicles and lithium-ion batteries used for portable electronics such as laptops and smartphones. Batteries come in many shapes and sizes, from miniature cells used to power hearing aids and wristwatches to small, thin cells used in smartphones, to large lead acid batteries used in cars and trucks, and at the largest extreme, huge battery banks the size of rooms that provide standby or emergency power for telephone exchanges and computer data centers. According to a 2005 estimate, the worldwide battery industry generates US$48 billion in sales each year, with 6% annual growth.

Batteries have much lower specific energy (energy per unit mass) than common fuels such as gasoline. In automobiles, this is somewhat offset by the higher efficiency of electric motors in producing mechanical work, compared to combustion engines. Figure 2-19 Shows the power requirement for deferent application

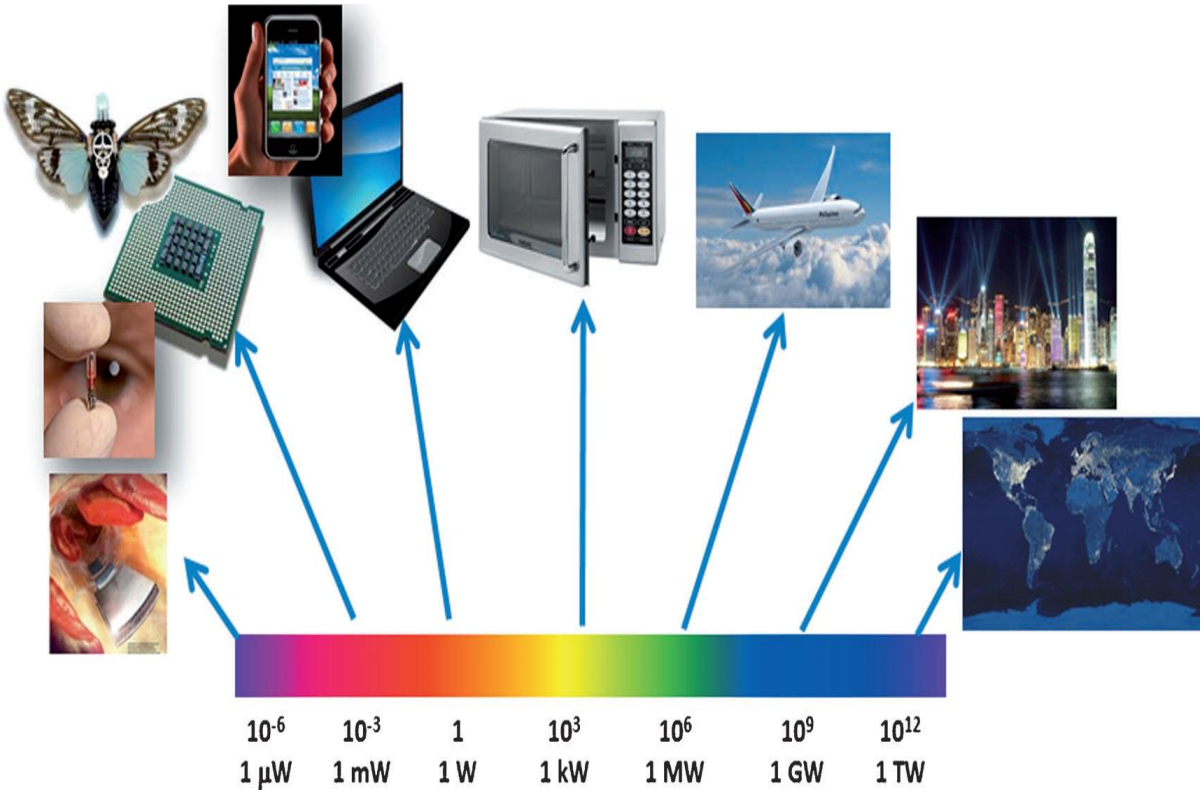

Figure 2-19 Power requirements for different applications

Table 2-4 show the most commonly used battery within the range:

Battery	Voltage (V)	Capacity (mAh)	Mass (g)	Volume (cm^3)	Specific Energy (Wh/kg)	Energy Density (Wh/l)
Energizer NH15-2450 NiMH AA	1.2	2450	30.00	8.34	98.00	352.52
Energizer NH22-175 NiMH 9V	8.4	175	42.00	21.52	35.00	68.31
Varta V15H NiMH button type	1.2	15	1.30	0.32	13.85	60.00
Samsung AB463446FZ Li-ion cell phone	3.7	800	17.90	8.36	165.36	354.07
AA Portable Power Corp. PL-383562-C2 Li-Polymer single cell	3.7	850	18.00	7.26	174.72	152.73
Front Edge Technology, Inc. NanoEnergy® Lithium thin-film	4.2	4	0.45	0.11	76.36	152.73
Infinite Power Solutions, Inc. Thinergy® MEC101-7 Lithium thin-film	4.0	0.7	0.22	0.11	6.22	25.45

We suggest the lithium thin film for the following reasons:

Table 2-4 rechargeable betters comparison

Conventional Batteries	Super capacitors	lithium thin film
+ High discharge current + High energy density + Inexpensive - Limited life - Replacement labor cost - Unsafe, polluting - Form factor	+ Peak power delivery + Long life + Inexpensive - High leakage - Very low energy density - High temperature degradation - Form factor	+ High discharge current + High energy density + Near Zero Leakage + Long life / Permanent + Low cost of ownership + Form factor + Safe / Eco-Friendly + Broader Temp Range

For example, MEC201 (lithium thin film) vs. CR2032 (Li Coin Cells). A single MEC201 delivers the same lifetime capacity as 45 coin cells. A single MEC201

delivers the same capacity in the first 220 charge cycles. Figure 2-20 shows MEC201 (lithium thin film) vs. CR2032 (Li Coin Cells)

Figure 2-20 MEC201 (lithium thin film) vs. CR2032 (Li Coin Cells)

2.10 Control System Based On RC

A radio-controlled aircraft (often called RC aircraft or RC plane) is a small flying machine that is controlled remotely by an operator on the ground using a hand-held radio transmitter. The transmitter communicates with a receiver within the craft that sends signals to servomechanisms (servos) which move the control surfaces based on the position of joysticks on the transmitter. The control surfaces, in turn, affect the orientation of the plane.

Flying RC aircraft as a hobby grew substantially from the 2000s with improvements in the cost, weight, performance and capabilities of motors, batteries and electronics. A wide variety of models and styles is available.

Scientific, government and military organizations are also using RC aircraft for experiments, gathering weather readings, aerodynamic modeling and testing. Unmanned aerial vehicle (drones) or spy planes add video or autonomous capabilities, and may be armed.

The basic components of a typical radio control system are the transmitter, receiver and servos. Battery packs, or individual cells, are needed to power all the components. However, receivers and servos of modern Electric Power (EP) RC airplanes don't usually have their own battery pack because their power is taken directly from the motor battery pack via what's known as a BEC Traditional MHz radio control systems were commonly purchased as a complete set that included

the transmitter, receiver, 4 standard servos and a battery charger .Figure 2-21 shows the component of RC

Figure 2-21 RC compnants

2.11Electromechanical Modeling of Piezoelectric Harvester

The source of mechanical energy can be a moving human body or a vibrating structure. The frequency of the mechanical excitation depends on the source: less than 10Hz for human movements and over 30Hz for machinery vibrations (see Table 2-1).

Such devices are known as kinetic energy harvesters or vibration based power generators. From dynamic point, the piezoelectric can be equivalent as a damped mass-spring mechanical system by a linear time-invariant second order differential equation, as shown in Figure 2-22.

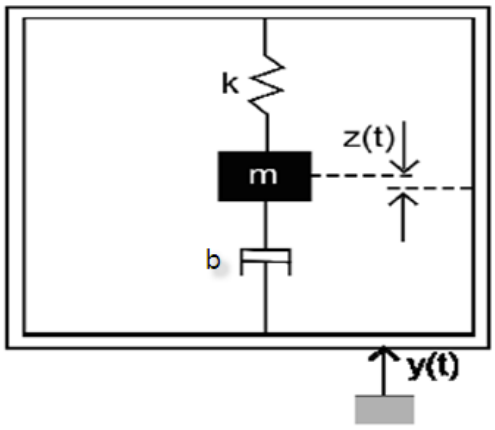

Figure 2-22Generic model of piezoelectric energy harvester

Where m, b, k is effective mass, damping coefficient, structure stiffness respectively. It is assumed that the mass of the vibration source is much greater than the mass of seismic mass in the generator and the vibration source is unaffected by the movement of the generator. Then the differential equation of the movement of the mass with respect to the generator housing from the dynamic forces on the mass can be derived as follows

$$m.\frac{d^2z(t)}{dt^2}+b.\frac{dz(t)}{d(t)}+k.z(t)=-m.\frac{d^2y(t)}{dt^2} \tag{2-3}$$

Rewritten 2-3in the form of Laplace transform as

$$m.s^2.z(s)+b.s.z(s)+k.z(s)=-m.a(s) \tag{2-4}$$

$$a(t)=\frac{d^2y(t)}{dt^2} \tag{2-5}$$

Where *a(t)* is acceleration of the vibration. The transfer function of vibration micro generation is

$$\frac{z(s)}{a(s)}=\frac{1}{s^2+\frac{b}{m}s+\frac{k}{m}}=\frac{1}{s^2+\frac{\omega_r}{Q}s+{\omega_r}^2} \tag{2-6}$$

Where resonant frequency ω_r and quality Q factor are given by

$$\omega_r=\sqrt{\frac{k}{m}},\mathrm{Q}=\sqrt{\frac{km}{b}} \tag{2-7}$$

Equivalent electrical circuit can be represented as shown in Figure 2-23.

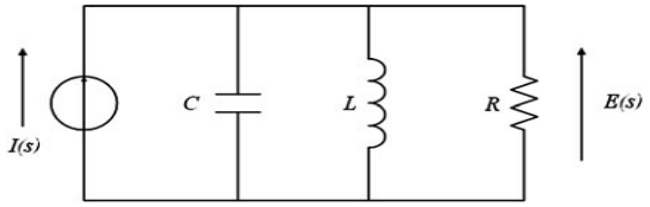

Figure 2-23 Equivalent circuit of kinetic energy harvesters

By comparing between the equation of an equivalent electrical circuit and kinetic energy harvester can be found

$$-m.a(s) = s.z\,(s)(\mathrm{ms}+\mathrm{b}+\frac{k}{s}) \tag{2-8}$$

Equivalent electrical circuit equation can be rewrite as

$$-I\,(s) = E\,(s)(sc + \frac{1}{R} + \frac{1}{sL}) \tag{2-9}$$

Where

$$I\,(s) = m.a(s), \mathrm{E(s)} = \mathrm{s.Z(s)}, \mathrm{C} = m, R = \frac{1}{b}, L = \frac{1}{k} \tag{2-10}$$

2.12 Previous studies

One of the earliest published works in vibration energy harvesting with piezoelectric materials was presented by Taylor and Burns [3] in which they proposed the use of an array of Poly Vinylidene Flouride (PVDF) Piezoelectric polymer film to harvest hydrodynamic energy from ocean waves. Although no physical system was proposed or built, it was theorized that a 100 MW power plant utilizing PVDF could deliver power to an onshore grid at a cost of 2.5 cents per kWH. The following year, Häsler, et al. [4] performed what appears to be the first experimental study using piezoelectric materials to harvest energy. They proposed the use of a PVDF film as an implantable power source in a biological system. A prototype device was fabricated and implanted in vivo into the ribcage of a dog to harvest energy available from the relative motion of the ribs during breathing. Experimental testing showed that the PVDF harvester could generate a peak voltage of 18 V, corresponding to about 17 W of power, which was short of

the predicted 1mW goal. Three years later Hausler and Stein [5] published a work in which PVDF film was again proposed for use in harvesting

At the start of the 21st century, a surge of research involving piezoelectric energy harvesting occurred. Since the year 2000, hundreds of papers have been published exploring various aspects of vibration energy harvesting using piezoelectric materials including the development of electromechanical models of piezoelectric harvesters, the efficiency of various piezoelectric materials and harvester configurations, energy harvesting circuitry, and various harvesting applications including micro electromechanical systems (MEMS), self-powered sensors, and biological systems. Several articles highlighting the work in piezoelectric energy harvesting in the last years are reviewed in the following. An incessant interest has been placed by the research community on the development of electromechanically coupled models that can predict the behavior of a piezoelectric energy harvesting system with increasing accuracy. Many of the early modeling efforts utilized a simple model of an electromagnetic harvester developed by Williams and Yates [6]. The model was developed to describe electromagnetic harvesting; therefore, its use is highly inaccurate in modeling piezoelectric transduction. To improve upon the existing models, Roundy and Wright [7]and DuToit and Wardle [8]both presented single-degree-of freedom (SDOF) lumped parameter models of piezoelectric energy harvesters. Although the lumped-parameter solution showed improvement over the Williams and Yates [6]it is limited to describing a single vibration mode and lacks much of the information necessary to accurately describe the coupled system. In an effort to further refine the piezoelectric harvester models, discrete Rayleigh-Ritz formulations (originally developed by Hagood, et al. [9]for piezoelectric actuation) were developed for Euler-Bernoulli cantilever beam harvesters by Sodano, et al. [10]and DuToit and Wardle [8] later improved upon by Elvin and Elvin [11]The Rayleigh-Ritz formulation provides a discretized approximation (having finite degrees of freedom) of the distributed parameter system and yields more accurate approximations than SDOF models. More recently, Erturk and

Inman [12] have presented the exact electromechanical solution of a cantilever piezoelectric energy harvester under harmonic base excitation based on Euler-Bernoulli beam assumptions. The exact analytical solution provides the most accurate model of cantilevered piezoelectric vibration energy harvesting. Additionally, Erturk and Inman [13]have also presented improved approximate distributed parameter modeling of piezoelectric energy harvester beams that can be used to model non uniform beams where an exact solution does not exist.

Significant interest has also been placed on improving the efficiency and practicality of piezoelectric harvesting through the investigation of various piezoelectric materials as well as physical configurations of vibration energy harvesters. The most common material used in piezoelectric energy harvesting is lead ZIRCONATE TITANATE (PZT), which is a piezoelectric ceramic. Although widely used in energy harvesting applications, PZT is extremely brittle; causing limitations in the strain that can be applied to the material without causing Damage. For this reason, researchers have investigated other, more flexible materials for vibration harvesting. Sodano, et al. [14]compared the energy harvesting performance of monolithic piezo ceramic to more flexible piezoelectric composite and fiber-based devices Including Macro Fiber Composites (MFCs) and Quick Pack R actuators. Lee, et al. [15]and Taylor and Burns [3] both explored the use of PVDF film for energy harvesting applications.

wang [16] present method of using piezoelectric material inside active CT and MRI to move the patient precisely inside it

teams [17] have developed a prototype mobile device charging t-shirt that uses Piezoelectric film to convert sound waves into electric charge, the Sound Charge t-shirt prototype's modified A4-sized panel of Piezoelectric film at the front is said to act like an oversized microphone, absorbing sound waves and converting them via the compression of interlaced quartz crystals into an electrical charge. This is then fed into a small external reservoir battery (with visuals that pulse in time with the music) and the wearer can then pop a mobile phone or

smartphone into the pocket above the panel, connect it up to the reservoir and top up the device battery using sound.

Pratihari [18] make a research under the name of PIEZOELECTRIC CAR Each of these piezoelectric car tires is equipped with an array of highly bendable PZT benders covering most of the inner surface. The output due to deformation of tires, which is an A waveform has to be converted into DC signal by a rectifier before it can be cached in a capacitor. Each row of benders, running across the width of tire is taken as one generator & is rectified separately with all PZT lines connected in parallel. At any given time only three or four rows, depending on the length of AN ARRANGEMENT OF the contact patch, generate power. PZT BENDERS IN A TIRE

Zhao [19] studies a piezoelectric energy harvester for the parasitic mechanical energy in shoes originated from human motion. The harvester is based on a specially designed sandwich structure with a thin thickness, which makes it readily compatible with a shoe. Besides, consideration is given to both high performance and excellent durability. The harvester provides an average output power of 1mW during a walk at a frequency of roughly 1 Hz. Furthermore, a direct current (DC) power supply is built through integrating the harvester with a power management circuit. The DC power supply is tested by driving a simulated wireless transmitter, which can be activated once every 2–3 steps with an active period lasting 5ms and a mean power of 50mW. This work demonstrates the feasibility of applying piezoelectric energy harvesters to power wearable sensors.

In the past few years, piezoelectric vibration harvesting has gained interest for use in UAVs as a means of harvesting energy from vibrations persistent during the flight of the aircraft in order to create local power sources for low-power electronics. Previous research studies have investigated several aspects of harvesting vibration energy in UAVs using piezoelectric material.[20] [21] explored the use of piezoelectric harvester plates on the wings of UAVs for harvesting vibration energy during flight. An electromechanically coupled finite element model was developed for piezoelectric plates that can be used to predict

the energy output of harvester plates in UAVs. Both theoretical and experimental validation was performed on the finite element model against the analytical solution presented By Erturk [22] and against experimental test results of a cantilever harvester plate also presented by Erturk [23]. Additionally, a case study was presented in which theoretical optimization was performed on a UAV Wing spar model. Results of this work proved the effectiveness of the finite element model in predicting the behavior of cantilever piezoelectric harvester plates as well as the ability to determine an optimal amount and optimal location of piezoelectric material in a UAV wing spar. In a continuation study, De Marqui Jr [20] coupled their previously developed finite element model with an unsteady aerodynamic model and investigated the effects of airflow excitation on the power output of cantilever piezoelectric energy harvester plates which simulate the wing of a UAV. Various airflow speeds as well as electrode configurations of the piezoelectric (segmented electrodes vs. continuous electrodes) were analyzed. Results showed that energy harvesting performance is optimized for airflow speeds near the flutter speed, although impractical for actual flight situations, and that segmented electrodes can be useful in eliminating voltage cancellation experienced under torsional vibrations. Perhaps one of the more promising uses of piezoelectric energy harvesting in aircraft is in providing power to low power sensor nodes. Several researchers have investigated the possibility of utilizing vibration energy harvesting in aircraft to create self-powered structural health monitoring nodes that are capable of assessing the condition of critical aircraft components during flight. Durou and A. [24]investigated the combination of thermal and vibration harvesting to power SHM sensors on large-scale aircraft. Simulations were performed to predict the power output of both harvesting devices as well as the energy storage performance of a super capacitor used to store the harvested energy. Results of the simulations suggest that vibration harvesting alone is not suitable to directly power the SHM node, but that it acts as a valuable supplement to the solar harvesting system as the output of the piezoelectric harvester is not environmentally dependent. Moss [25] explored the

concept of broadband vibration energy harvesting in aircraft to provide power to SHM sensor nodes. Considering the variability in excitation characteristics during the flight of an aircraft, it was proposed to develop an energy-harvesting device with 18 relatively broadband responses. A large vibrio-impacting device was created and experimentally tested, in which a vibrating mass repeatedly impacts and excites a piezoelectric beam. The mass responds to a range of frequencies, thus the overall device is capable of harvesting energy in a broadband sense. Results of experimental testing showed that the harvester responds in the range of 29 - 41Hz and is capable of harvesting up to 12mW of power under 0.5g excitation. Featherston [26] performed research on vibration energy harvesting for SHM sensors on both large scale commercial aircraft as well as small UAVs. A test panel was created using an aluminum plate clamped on all edges in a test Frame and included four surface mounted piezoelectric devices for energy harvesting. The panel was excited using a shaker with a stinger connection at the center of the plate for various frequencies corresponding to different air speeds, altitudes, and panel locations along the wing. Results of experimental testing showed that the maximum power harvested by a single device was 23.5mW. In order to operate a SHM sensor node requiring 50mW of power, it was concluded that approximately 71cm2 of piezoelectric material is required under optimal conditions.

Many novel UAVs include a multitude of functions requiring a large amount of technology to be placed into a small platform. The concept of multifunctional piezoelectric energy harvesting has been investigated in the literature as a means of creating a noninvasive power source that can be used, for example, to power on board self-powered electronic systems. Apker [27] suggested the use of piezoelectric film on the wings of a small ornithopter flapping-wing MAV to perform aero elastic energy harvesting during Flight. The piezoelectric material would serve as both a load bearing wing surface as well as an energy harvesting system, hence its multifunctional use. Although no modeling efforts were pursued and no physical device was constructed, the work presents a novel concept in

multifunctional harvesting for UAVs. Another novel concept for multifunctional Piezoelectric vibration harvesting in UAVs involves the integration of piezoelectric Material into the landing gear of the aircraft. Magoteaux [28] discussed the concept of using either cantilevered or curved piezoelectric beams as the landing gear for UAVs.

Piezoelectric landing gear can be used not only for conventional takeoff and landing purposes, but to harvest energy and recharge the power source during a mission if the aircraft is perched on a vibrating structure. In their work, Magoteaux et al. provided a comparison of the harvesting ability of a traditional piezoelectric cantilever to a curved piezoelectric 19 configurations and found that while having potential to provide larger amounts of power (5mW at 1.0g), the resonance frequency of the cantilever configuration is impractically low (3.5Hz) compared to the curved configuration (120Hz), thus the curved device, which provides around 3mW, is best suited for landing gear applications. In a similar

Study, Erturk [23] investigated a novel L-shaped configuration for piezoelectric energy harvesting and suggested its use as UAV landing gear. The L-shaped beam mass structure can be tuned to exhibit a two-to-one internal resonance phenomenon where the second resonance frequency is roughly two times the first, and has potential for giving larger power outputs compared to traditional cantilever configurations. Additionally, an L-shaped device is well suited geometrically for use as landing gear. Erturk et al. compared the energy generation capabilities of their proposed L-shaped device to the curved Harvester proposed by. Magoteaux [28] and found that for devices with similar dimensions and mass, the L-shaped device outperforms the curved device. Anton [1] designed a UAV with impeded spar covered by piezoelectric harvester at addition to solar panel on the top of wings to generate power from the vibration of the spar.

From the Literature Review and Related Works review noted that a multifunctional approach is paramount as the size of UAVs continues to decrease and the technological demands steadily increase. the output generated power is at various values depend on the effected vibration and the required function from

the harvested power when the piezoelectric material act as power generator or on value of electrical power are available and the required movement when the piezoelectric material act as actuator. at most the previous designs the output power is not high enough to be used at useful function in the system.

Most of researches focus on integration of vibration energy harvesting systems into unmanned aerial vehicles to provide environmentally independent power sources for just the small onboard sensors. Finally, the location of the power generator, sometimes located on non-modular part of UAV (e.g. spar) so it will be difficult to be maintain. Unfortunately, the studies are very rear in this filed.

3 CHAPTER THREE

SYSTEM DESIGN

3.1 Introduction

The process through which the system will work at maximum allowed performance is shown in Figure 3-1.The wigs selection is the first step it controlled by many criteria (aspect ratio , cruse speed ,physical characteristic ,air foil shape ,and availability).The aspect ratio of a wing is the ratio of its span to its mean chord In the field of piezoelectric power generation the best wing type is that one have the highest aspect ratio to its flexibility and to get the highest wing flexibility it better to fly near to the flutter speed and that is also can be applied by the high AR wings on very low velocity. The cruse speed is a speed on the flight phase. It depends on the type of wind but usually on the highest speeds the harvested power will be more than the lower so it's better to select airfoils that con fly at high speeds. Wing physical characteristic: this criterion can't be neglected at all. the wings dimensions and weights is related to the above and also effect on the flutter and the natural frequency(Natural frequency is the frequency at which a system tends to oscillate in the absence of any driving or damping force.) for the safety of aircraft the frequencies of each velocity must be determined to avoid the matching between the vibration generated by aerodynamic forces and the natural frequency on the wing it self .the result on the matching will generate a huge damage on the structure . Based on the above criteria the selected wing will tested in Wind tunnel equivalent model to calculate Pressure distribution on the wing. Figure 3-1 shows the process flow chart.

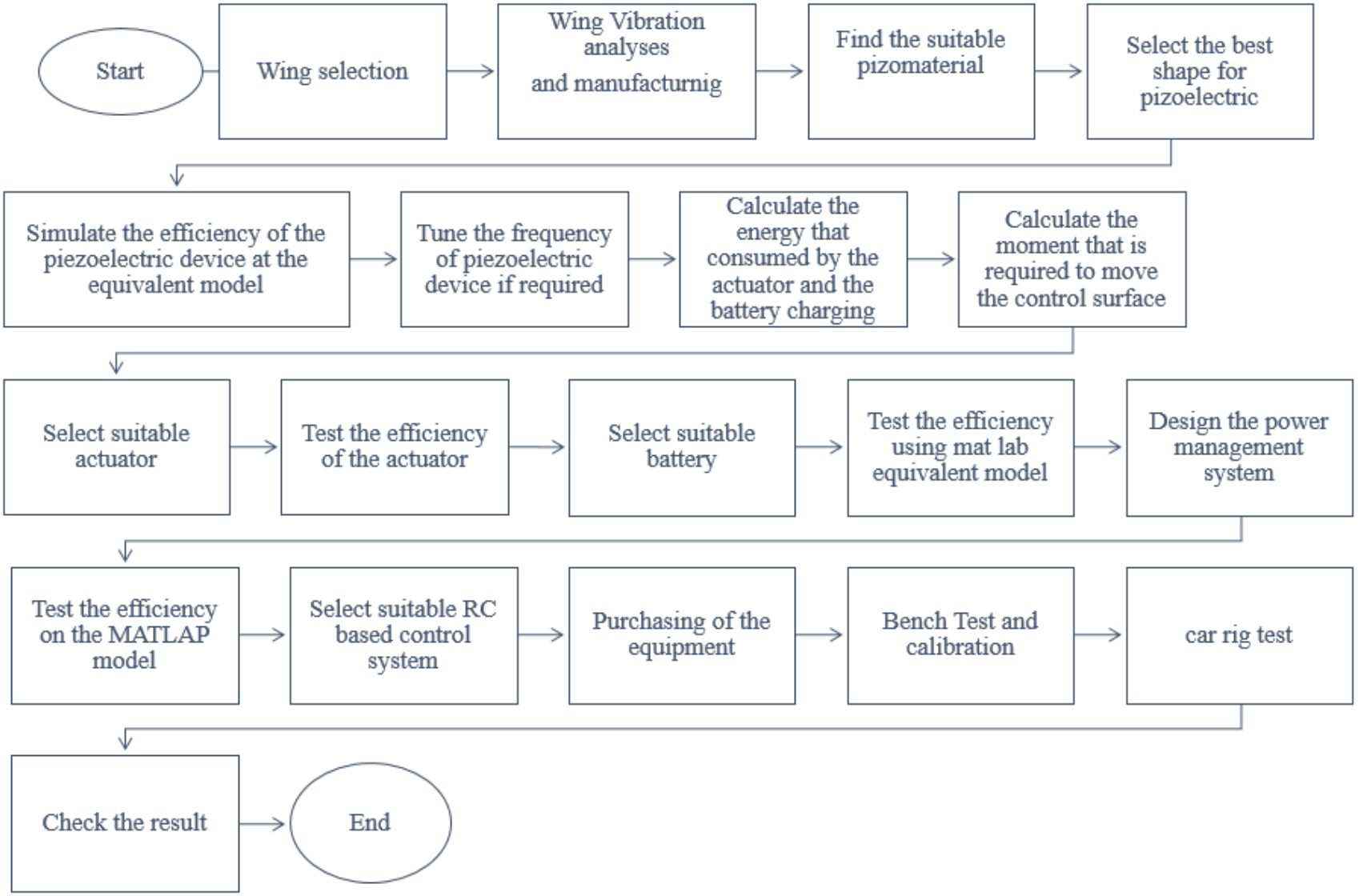

Figure 3-1 process flow chart

3.2 types of Wings and Their Specifications

3.2.1 NACA0012 Aero foils

As shown in Figure 3 2.the main specifications are:

- 300 mm span
- Chord 150 mm

Figure 3-2 NACA0012 Aerofoil

3.2.2 NACA2412 Aero foil with Variable Flap

As shown in Figure 3 3.the main specifications are:

- 300 mm span
- Flap adjustable by +/– 90 degrees
- Chord 150 mm

Figure 3-3 NACA2412 Aerofoil

3.2.3 NACA 2415 Aero foil

As shown in Figure 3 4.the main specifications are:

- Wingspan: 300
- Flap adjustable by +/– 90 degrees
- Chord 150 mm

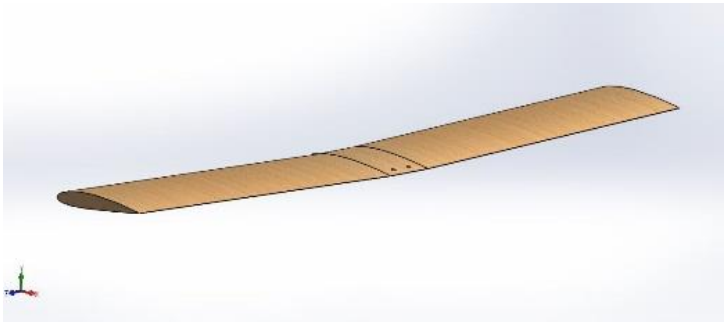

Figure 3-4 NACA 2415 Aerofoil

3.2.4 NACA 652415 Aerofoil

As shown in Figure 3 5.the main specifications are:

- Tip chord:0.190079
- Root chord:0.190079
- Wing span:0.8228

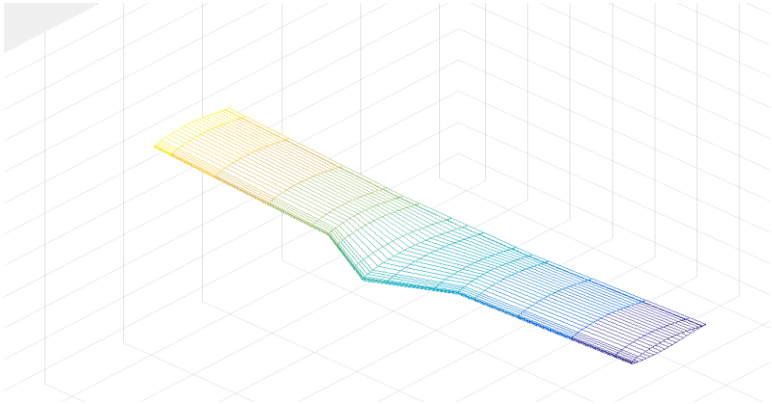

Figure 3-5 NACA 652415 Aerofoil

3.3 Selection criteria

The work core is to generate the heights energy value from the aerodynamic forces on the wing, first of all the availability of the product sometimes the best solution is well-known but there is a limitation on the manufacturing facilities. But generally the effect must be considered to select the wing shape aspect ratio

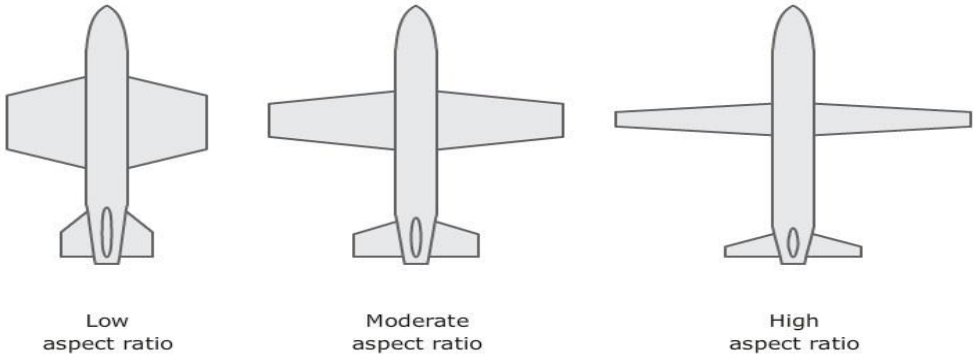

Figure 3-6 Aspect ratio effect on wing shape

The aspect ratio of a wing is the ratio of its span to its mean chord. It is equal to the square of the wingspan divided by the wing area. Thus, a long, narrow wing has a high aspect ratio, whereas a short, wide wing has a low aspect ratio. Other important factor is related to the AR is the flutter speed (Flutter is a dangerous phenomenon encountered in flexible structures subjected to aerodynamic forces. ... Flutter occurs as a result of interactions between aerodynamics, stiffness, and inertial forces on a structure.) Figure 3-7 shows the variation of flutter speed with increasing AR. The flutter speed decreases with increasing AR. The variation of flutter frequency with AR is shown in Figure 3-8 . The flutter frequency decreases with increasing AR.

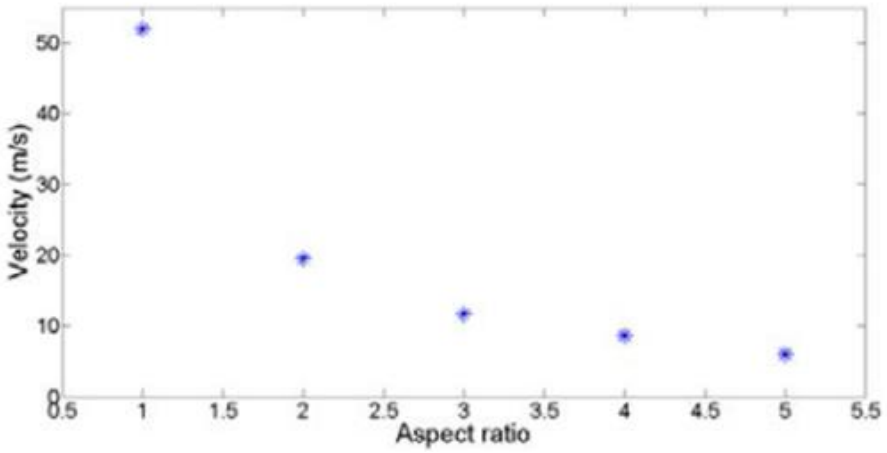

Figure 3-7 variation of flutter speed with increasing AR

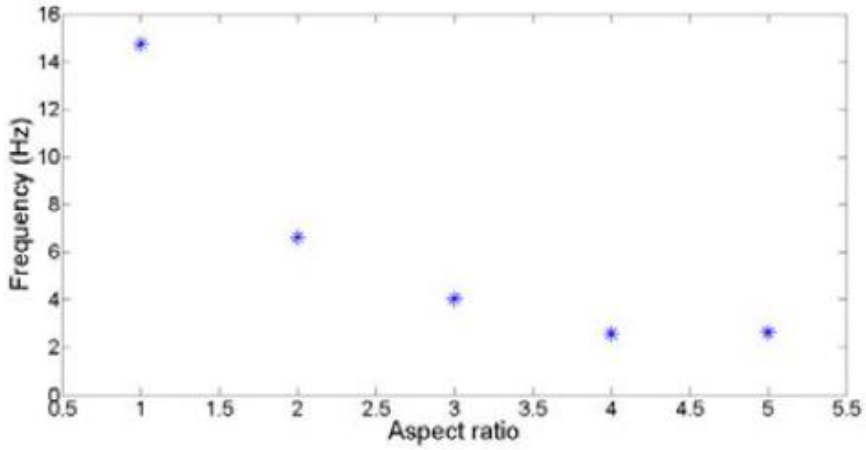

Figure 3-8 variation of flutter frequency with AR.

In the field of piezoelectric power generation, the best wing type is that one has the highest aspect ratio to its flexibility and to get the highest wing flexibility it better to fly near to the flutter speed and that is also can be applied by the high AR wings on very low velocity.

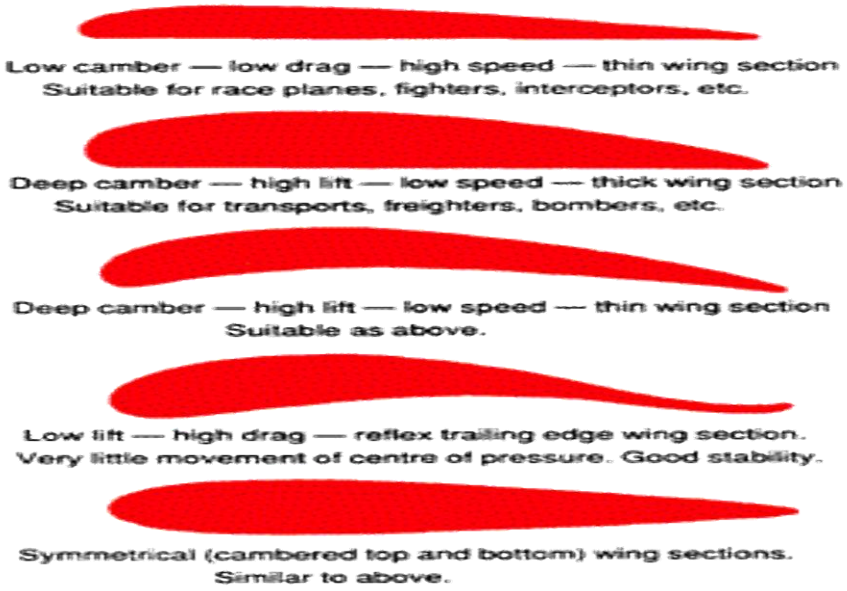

Figure 3-9 airfoils shapes

Secondly the cruise speed: the speed on the flight phase that occurs when the aircraft levels after a climb to a set altitude and before it begins to descend. It depends on the type of wind but usually on the highest speeds the harvested power will be more than the lower so it's better to select airfoils that can fly at high speed

Wing physical characteristic: this criteria cannot be neglected at all the wings dimensions and weights is related to the above and also effect on the flutter and the natural frequency (natural frequency is the frequency at which a system tends to oscillate in the absence of any driving or damping force) for the safety of aircraft the frequencies of each velocity must be determined to avoid the matching between the vibration generated by aerodynamic forces and the natural frequency on the wing it self .the result on the matching will generate a huge damage on the structure. Based on the above criteria the selected wing is NACA 652415 Aero foil. Figure 3-10 shows the elements of the best solution.

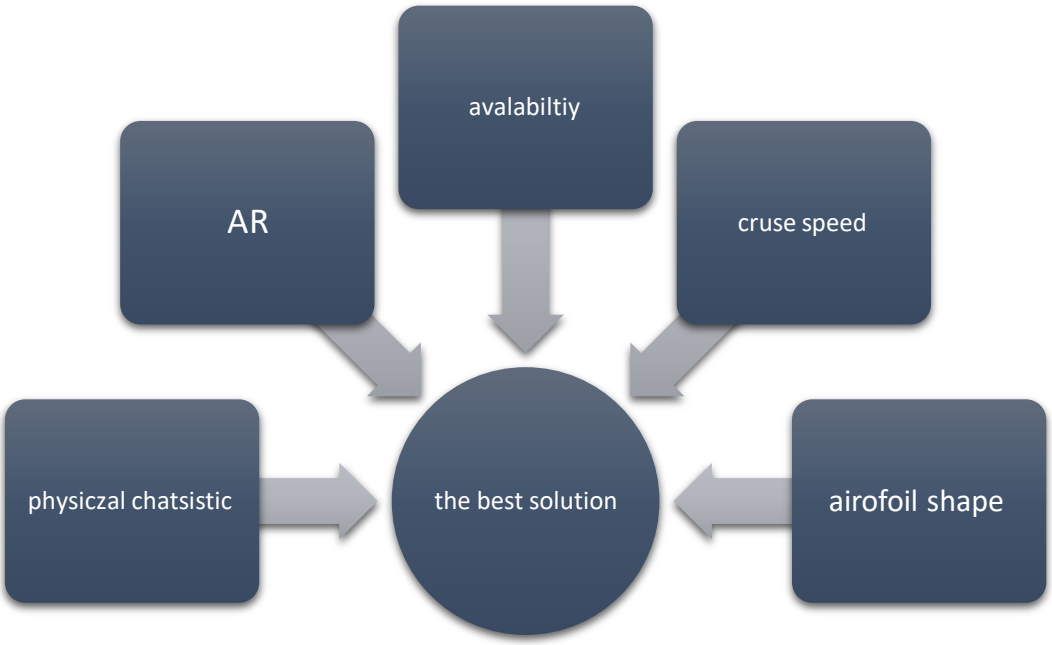

Figure 3-10 elements that effect on the best solution

3.4 Wind Tunnel Equivalent Model

The Wind tunnel is a tool used in aerodynamic research to study the effects of air moving past solid objects. A wind tunnel consists of a tubular passage with the object under test mounted in the middle. Air is made to move past the object by a powerful fan system but it's very costly to run wind tunnel test on the realty so the wind tunnel equivalent model is used to verify the results before the real test .the model that was use on the research is designed by professional engineers and it is verified by authorized doctors it is written by MATLAB program the inputs for the code are the geometry of the wing (root chores, tip cored ,span ,airfoil shape

,number of panels on a span wise and chord wise) .flight condition (air density on the wind tunnel ,flight speed ,angel of attack in fluid dynamics, angle of attack (AOA, or (Greek letter alpha)) is the angle between a reference line on a body (often the chord line of an airfoil) and the vector representing the relative motion between the body and the fluid through which it is moving). The wind tunnel that was selected to do the exponents have the following characteristic:

- Test section dimensions: 1.5 m (w) *1m (H)*3m (L)
- Speed:80m/s
- Type: close loop low speed wind tunnel

3.4.1 Pressure Distribution on the Wing

The pressure distribution on the wing is one of the result of the program it is shows the pressure destitution alone the wing. Table 3-1 shows the model data and Table 3-2 shows flight data.

Table 3-1 model data

Parameter	Value
Wing span	1.206m
Root chord	0.190079m
Tip chord	0.190079m
Airfoil	naca652415

Table 3-2 flight data

Flight speed	80m/s
Angle of attack	20degree
Air density	1.225Kg/m3

3.4.2 Panel method pressure distribution

The pressure is calculated at the center of each panel and arranged in a manner to be given at span wise station going around the airfoil at that station from trailing

edge to leading edge thorough the lower surface, starting from the left wing tip trailing edge going to leading edge, then to next station along the span.

Figure 3-11 show the Panel method wing geometry output

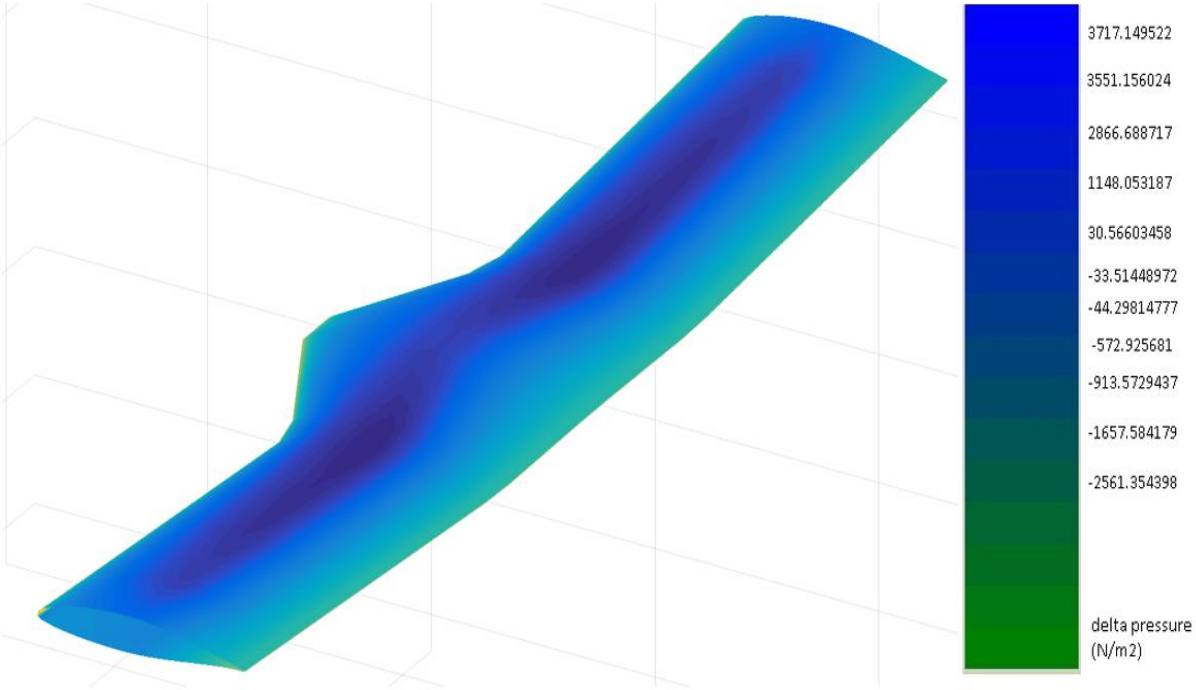

Figure 3-11 Panel method pressure distribution output

3.5 The frequency analyses

The output of the MATLAB code is applied to the ANSYS Workbench 16.0 software to do the Structure analysis, model analyses and the harmonic response. From the model analyses the shape mode and the natural frequency flutter speed was calculated and by the harmonic response the relation between the frequency and the wing displacement will define, the relation between the wing movement velocity amplitude meter per second and the frequencies of each speed was calculated, the directional displacement, normal stress and directional deformation are shown at Figure 3-13 and Figure 3-14

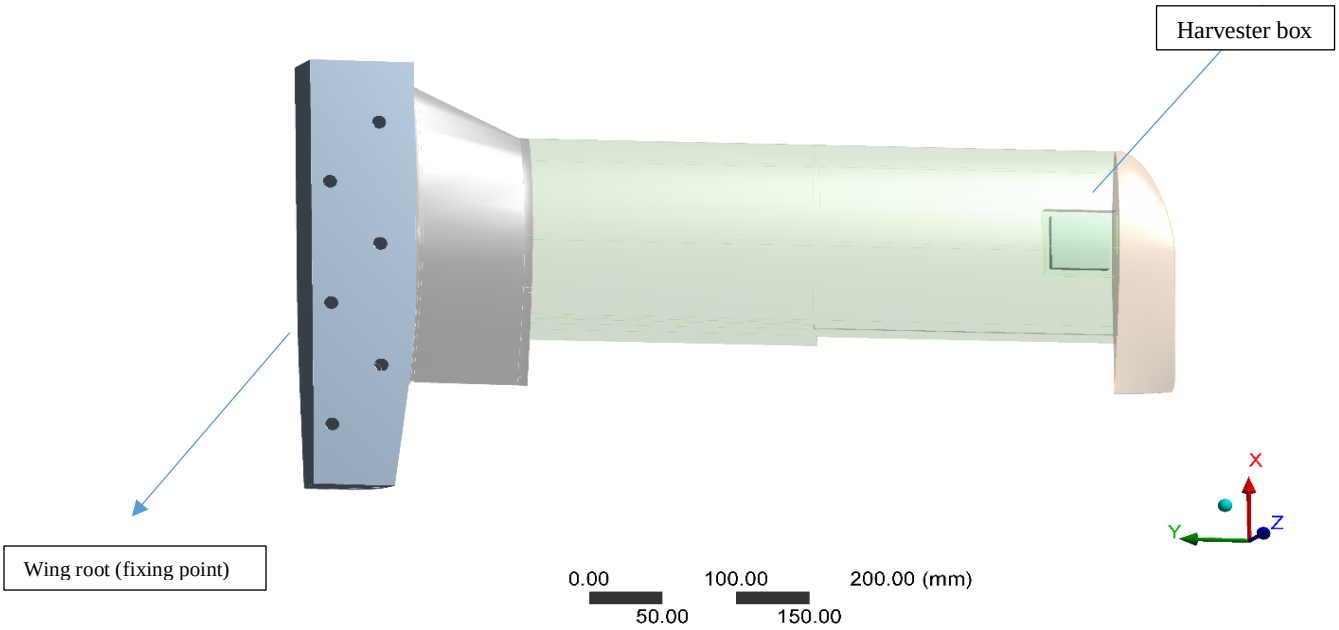

Figure 3-12 the wing with harvester inside

3.5.1 Structure Analysis:

The static analysis has been done to be sure that the structure has enough strength to endure the pressure without any failure. The analysis was made by ANSYS software (Static Structure Module). After importing the model into ANSYS environment and applying the boundary conditions such as load (the output of wind tunnel equivalent model) and fixed support, the results are revealed in Figure 3-13

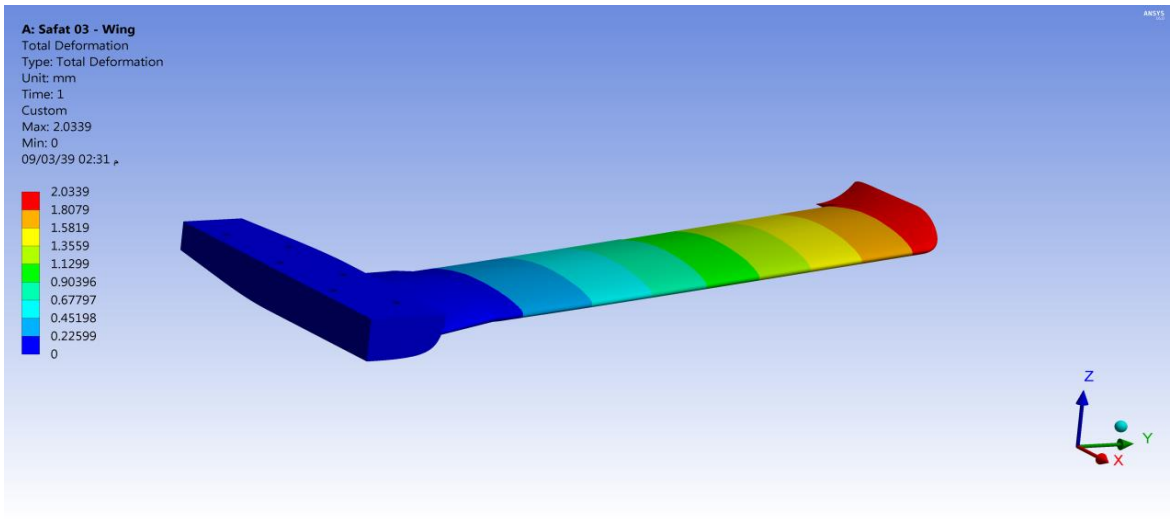

Figure 3-13: Total Deformation

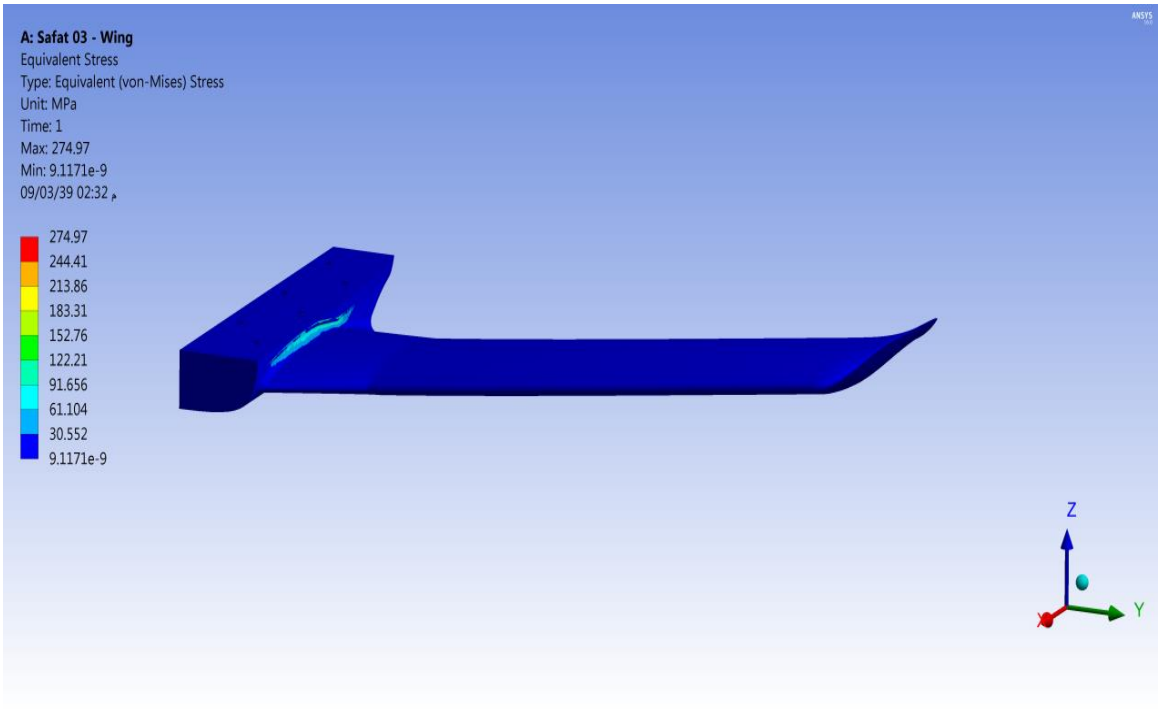

Figure 3-14: Distribution of Von-Mises Stress

It can be clearly seen that the maximum deformation is 2mm in Z direction. While as the maximum, stress according to von-misses is 275MPa, which located in the root.

3.5.2 Model Analysis:

After being sure that the model has a strong structure and can resist the aerodynamic load; the model analysis was, completed modal analysis is a technique to study the dynamic characteristics of a structure under vibrational excitation. Natural frequencies, mode shapes and mode vectors of a structure can be determined using modal analysis. Modal analysis allows the design to avoid resonant vibrations or to vibrate at a specified frequency and gives engineers an idea of how the design will respond to different types of dynamic loads. The objective of this Analysis is to determine the natural frequencies of the wing, study the mode shapes, subject the wing to a harmonic loading varying in frequency from zero – 600Hz, and study its response in terms of displacement and stress. The benefits of using ANSYS were that mode shapes could be accurately visualized and simulated. Therefore, the deformations occurring in the wing could be located with precision. A graphical variation of number of modes vs the frequency can also

be obtained from ANSYS Workbench. The results are illustrates in the figures at appendix B. Table 3-3 illustrate the frequency of each mode.

Table 3-3 modes vs frequencies

Mode	Frequency Hz
1	27.282
2	141.06
3	170.24
4	289.73
5	473.2
6	745.09
7	762.19
8	833.2
9	919.83
10	1125.3

The flutter speed of the wing was calculated using a simple method, which is based on an empirical investigation and calculates the torsional flutter. The method depends on torsion frequency, which was already calculated in the ANSYS analysis. Equation (3-1) to estimate the wing flutter speed to avoid it as follows.

$$V_T = 1.2 * C_{0.7} * f_T * \sqrt{A} \quad (3\text{-}1)$$

Where V_T is the flutter speed in m/s , $C_{0.7}$ is the wing chord length at 0.7b/2 in m, in which b is the wing span, f_T is the wing first torsion frequency in Hz, and A is the wing aspect ratio. Using data of Table 3-1 model data:

$$V_T = 1.2 * (0.7 * \frac{1.206}{2}) * 27.1 * \sqrt{(1.206/0.190)}$$

$$V_T = 34.58\, m/s$$

That means the test will be done in speed near to 34.85m/s. then the diving speed Vd and cruse speed Vd can be calculated Vc = Vd/1.25 and Vd = Vt/1.25 = 34.85/1.25=27.88m/s Vc = 27.88/1.25=22.30 m/s So Charging speed will be more than cruse speed and not at diving speed. It assumed to be at 25m/s = 90k/h and the frequency at this speed is 19.6hz

3.6 Finite element model for the harvester

The geometrical and physical parameters used in the simulation are given in Table 3-4 below

Table 3-4 Geometric and material parameters used in the simulation.

Parameters	Description	Values Units
L	Beam length	21 mm
b	Beam width	14 mm
hp	Piezoelectric layer thickness	0.06 mm
hs	Substrate layer thickness	0.04 mm
lm	End mass length	4 mm
lb	End mass width	14 mm
lh	End mass thickness	1.7 mm
Ys	Young's modulus of substrate material	209 GPA
Yp	Young's modulus of piezoelectric material	60.6 Gpa
ρs	Mass density of piezoelectric material (PZT-5H)	7500 kg/m3
ρp	Mass density of substrate material (Structural steel)	7850[kg/ m3]
ρm	Mass density of end mass material	7850[kg/ m3]
R	Load resistance	5k ohm

3.6.1 Geometry

A two dimensional geometry is considered for the simulation. The MEMS piezoelectric energy harvester has a cantilever with Rectangle mass at the tip, as shown in Figure 3-15. The device is made by a Structural steel covered with a piezoelectric layer on the two sides (up, down). The total length is 21 mm width is 14 mm consists of 3 parts the first parts r1 (1L*14W*1H) mm part 2 (21L*14W*0.16H) mm divided to 3 sup part 2 equal piezoelectric layers with diminution (21 L*14 W*0.06 H) mm and Structural steel layers with dimension (21 L*14W*0.04 H) mm part 3 (4 L*14 W*1.7 H) mm. Figure 3-15shows the Structure of piezoelectric energy harvester with tip mass

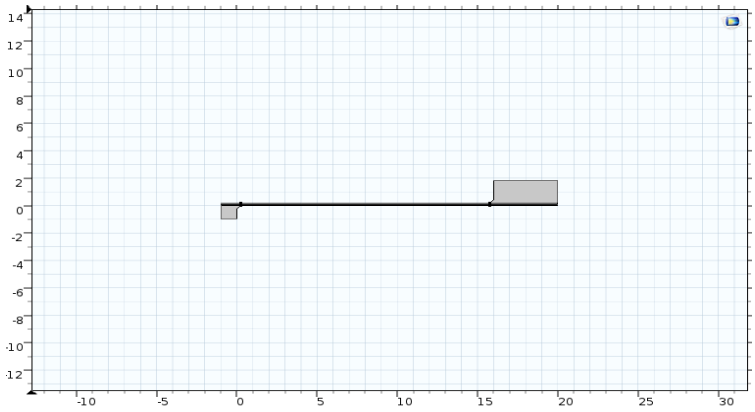

Figure 3-15 Structure of piezoelectric energy harvester with tip mass

3.6.2 Meshing

Figure 3-16 shows the meshing of piezoelectric energy harvester. The mesh is free triangular type with maximum element size 1.41mm and minimum element size 0.0063mm with resolution of narrow regions equal 1.

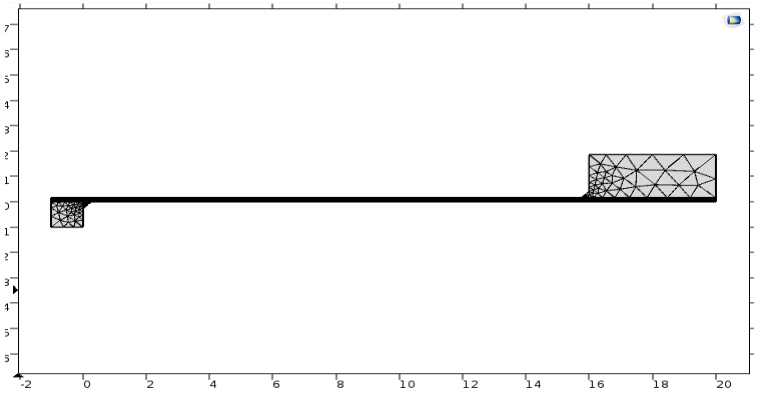

Figure 3-16 Piezoelectric Energy Harvester mesh.

3.6.3 Modeling results

Figure 3-17 Shows Total Displacement and stress of Piezoelectric Energy Harvester

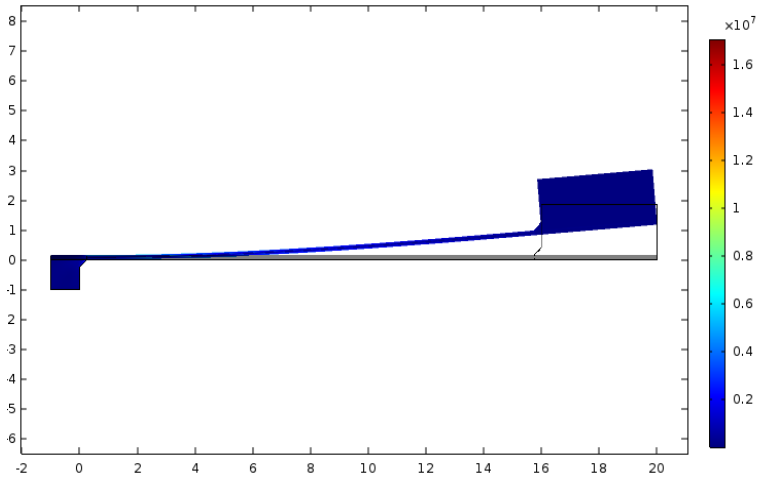

Figure 3-17 Total displacement and stress of piezoelectric energy harvester

Figure 3-18 shows frequency response

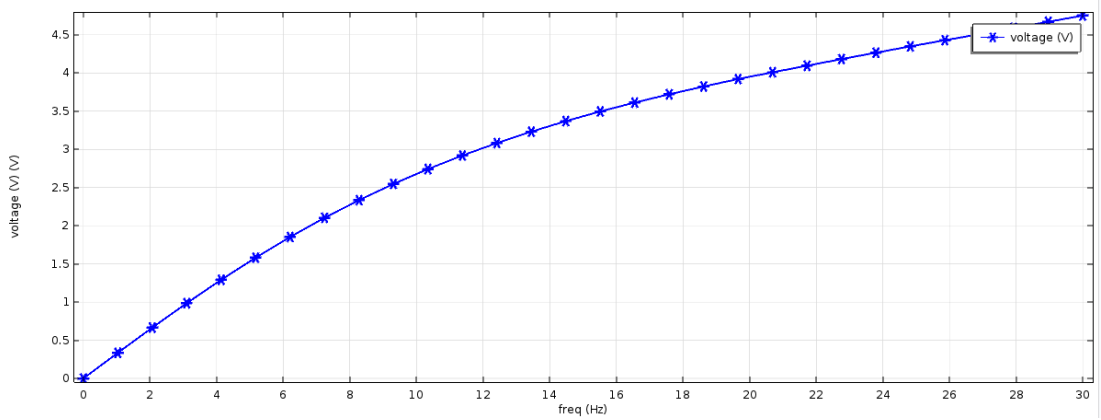

Figure 3-18 frequency response

From results above we found that the maximum Displacement is 3mm from the natural position and the stress is normal on the all element (below the ≈ 0.4 10^7n/m2) except on the attachment between the fixed point and the active piezoelectric layer ≈ 1.6 *10^7 n/m2 that is still normal. the maximum output voltage is 3.8 v on the frequency 19.6 /2g acceleration and the minimum is 3.6 on the frequency 17hz. the optimum R-load is 5kΩ.

3.7 Power Management Circuit

The simulation will be done for the all circuit. The input will be the harvester AC power that was harvested from the vibration source this power will be rectified

by 4-diode Bridge then it will be as input for the boot DC-DC converter to increase the output voltage and regulate it at constant level the output will feed the battery to study the charge and disgorge process.

The objective of this part to design boost converter that will have output equal 5 V from input voltage equal 3.9 v. the output ripple voltage less than one present. the load resistance is 5 kΩ, ideal components are assumed for this designee. By using the following MATLAB code, the power stage can be calculated.

```
%The following four parameters are needed to calculate
the power stage:
       % 1. Input Voltage Range: VIN(min)and VIN(max)
       %2. Nominal Output Voltage: VOUT
       %3. Maximum Output Current: IOUT(max)
       clc;
       disp('BOOST CONVERTER CALCULATION')
 Vin=input('enter the minimum input voltage:: ');
 Vin1=input('enter the maximum input voltage:: ');
 Vout=input('enter the output voltage:: ');
 I=input('enter the maximum output current:: ');
 fs=input('enter the switching frequency:: ');
 %calculation of maximum switch current
 n=0.9;
 D=1-((Vin*n)/Vout); %duty cycle
 di=.2*I*(Vout/Vin); %inductor ripple current
 L=(Vin*(Vout-Vin1))/(di*fs*Vout); %inductor value
 %dv=(I/(1-D))+(di/2);
 dv=0.5;
 C=I*D/(fs*dv);%output capacitor value
 R=Vout/I;
 disp('******************************')
 disp('DUTY CYCLE::::')
```

```
D=D*100;
D
disp('RIPPLE CURRENT:::')
di
disp('INDUCTOR VALUE:::')
L
disp('VOLTAGE RIPPLE:::')
dv
disp('CAPACITOR VALUE micro farad:::')
C=C;
C
R
disp('****************************')
```

Figure 3-19 shows boost converter MATLAB Simulink

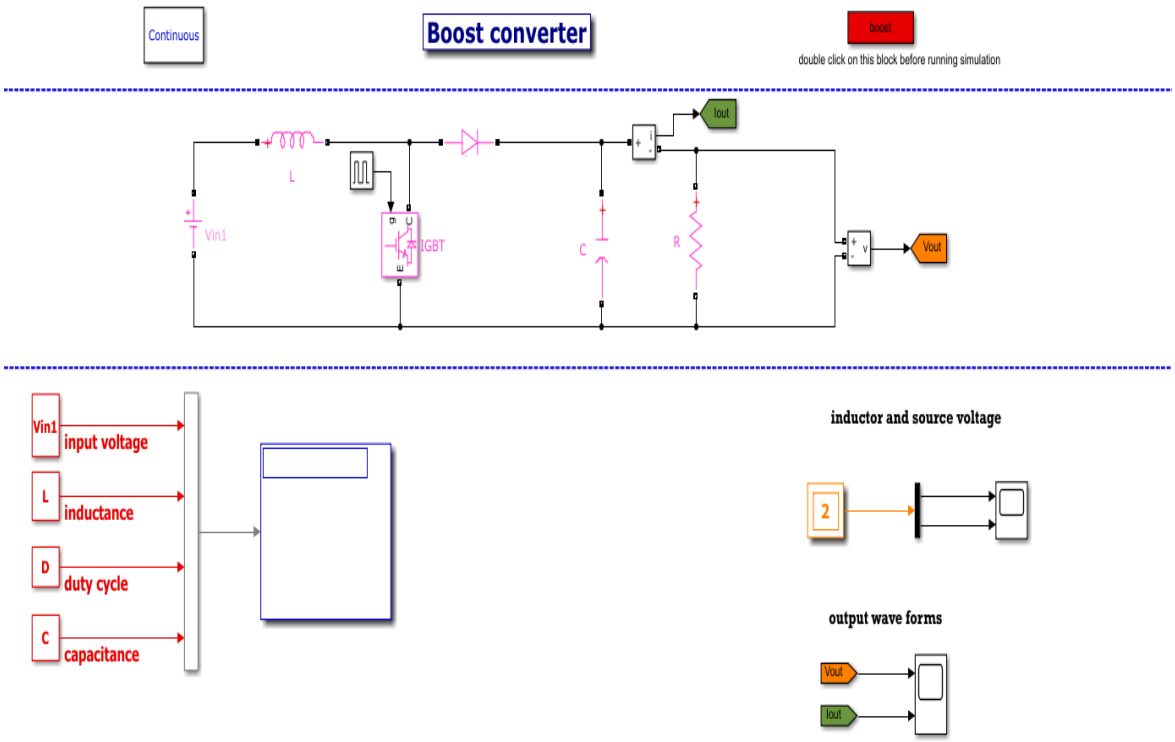

Figure 3-19 boost converter MATLAB Simulink

The Boost converter calculation as follows:

- Minimum input voltage: 3.6V
- Maximum input voltage: 3.8V
- Output voltage: 5V
- The maximum output current: 1A
- Switching frequency: 20000hz
- Duty cycle: d = 37.
- Ripple current: di = 0.2857a
- Inductor value: l = 1.3475e-04h
- Voltage ripple: dv = 0.5000v
- Capacitor value: c =3.7000e-05μF
- R = 5Ω

4 CHAPTER FOUR

RESULTS AND DISSECTION

4.1 Wing Manufacturing

The wing manufacturing process is consisting of three steps, as follows:

4.1.1 Bill of tools and materials

Table 4-1 shows material and tools quantity and specification

Table 4-1 material and tools quantity and specification

Materials		
Name	Quantity	Notes
E Glass Fabric	10m	0.5mm thickness for mold 2mm thickness for wing skin
Epoxy Resin	4L	With its hardener
Mosco Wood	0.03 *3m	Used as spars inside the wing
Car Polish	1 Pack	-
Cork	2*0.8m	-
Screws	-	-
Painting	-	-
Clay Clay	-	-
Iron Pipe	2m	-
Wires	2m	-
Control Horn	1	-
Emery Papers	1m	-
Tools		
Hot Ware	1	-
Drilling Tool	1	-
Cutting Tools	-	-
Paint Brushes	6	-
Keys	-	-

Emery Tool	1	-

4.1.2 master model manufacturing

Master model is the shape the is used to manufacture the wing mold. Figure 4-1 shows the makings process starting from print out 2D draft then using the wood to airfoil formation which is used to make the crock cutting more accurate and use it as guide to the hot war to find it way inside the cork. Then the output will be a cork with the shape of airfoil but need some emery to be smooth by applying the above proses again for the outer part of the wing full mater model will be ready for step three.

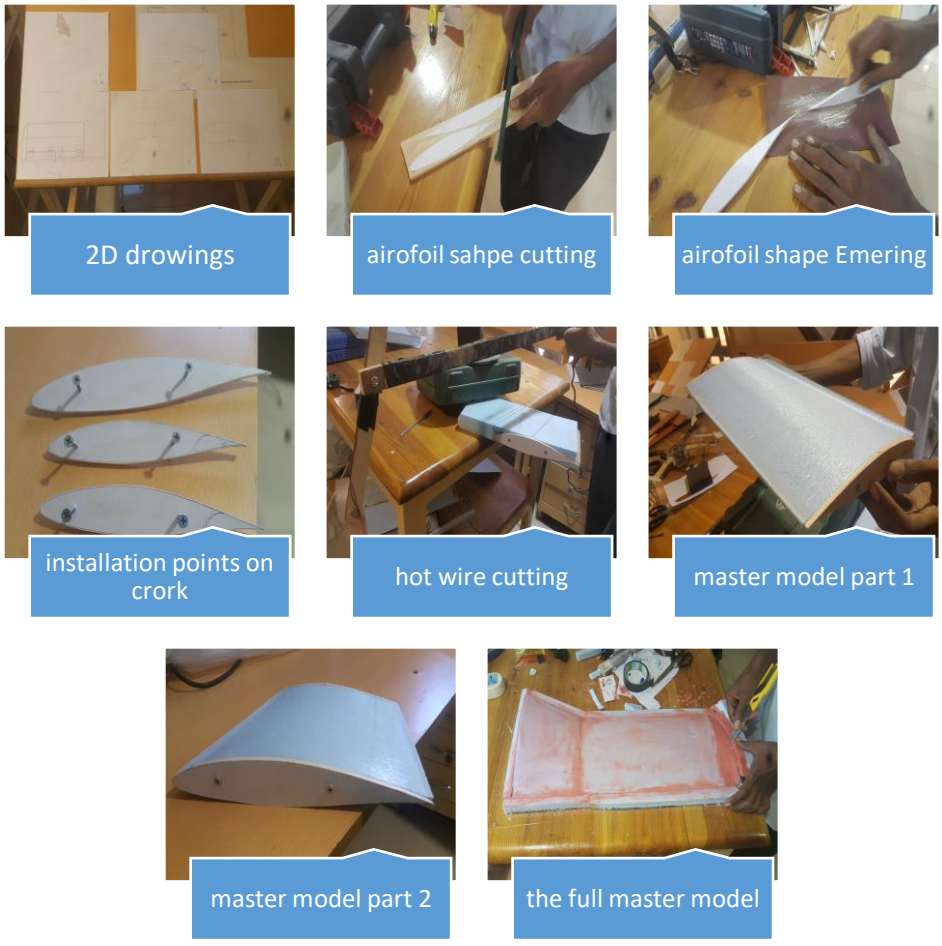

Figure 4-1 master model manufacturing process

4.1.3 wing mold manufacturing

It is the proses of making the wing mold, which is used to manufacture the wing itself with any numbers of products. the Figure 4-2 illustrates the mold manufacturing process which is started by using the cork master model as mold to

wing mold. using the painting brush to apply a skin of E Glass Fabric (2mm thickness) and Epoxy Resin on the cork model after using oil isolation between them after the fiber skin dray out then apply the same process three times (three layers). then repeat again for the mold lower side after that join the both sides together and fixing them with screws using drilling tool. Finally, after the mold dray out the both sides will be separated from each other and the mold will be ready for last step (wing manufacturing).

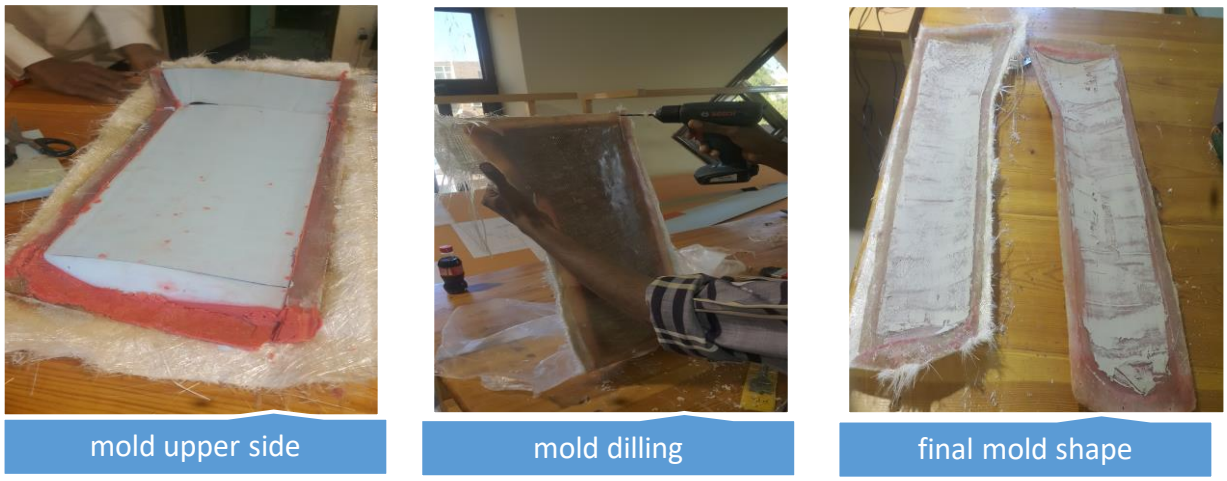

Figure 4-2 wing mold manufacturing

4.1.4 Wing Manufacturing

It is the proses of making the wing, the figure below illustrates the wing manufacturing process which is started using the painting brush to apply a skin of E Glass Fabric (0.5 mm thickness) and Epoxy Resin on the mold after using oil isolation between them. After the fiber skin dray out then apply the same process three times (three layers). The Mosco Wood 0.03 mm was inserted inside the wing skin to add more strength to the wing skin. then repeat again for the wing lower side after that join the both sides together and fixing them with screws. After the wing dray out the access doors and flab control surface are crated on the wing after finishing process the wing was painted.

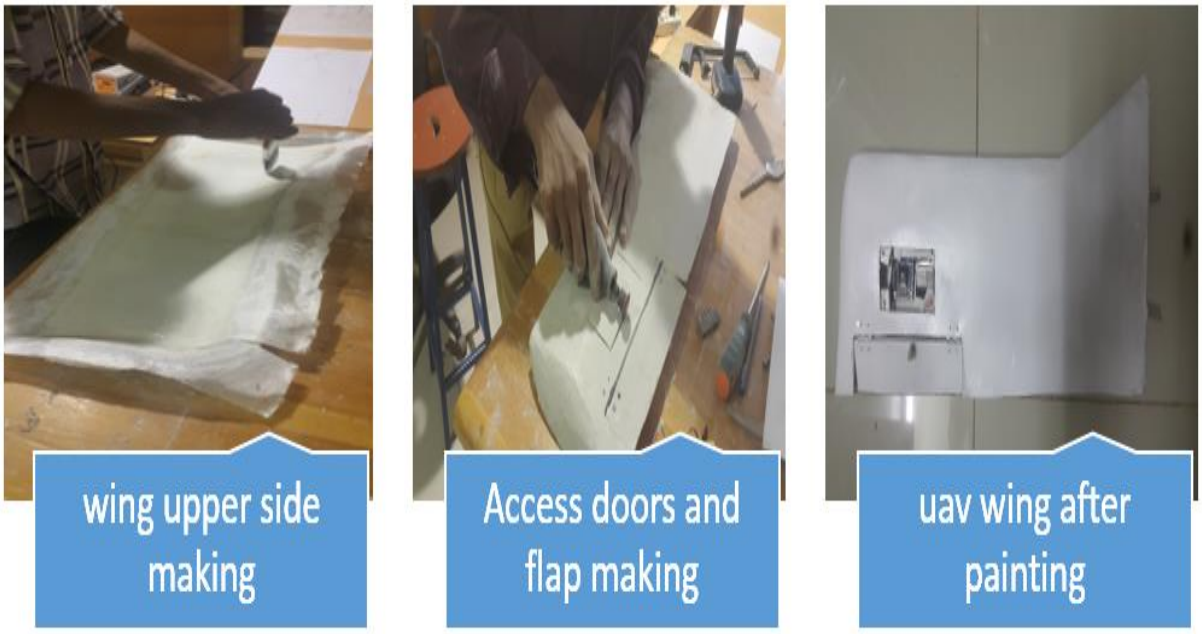

Figure 4-3 wing manufacturing

4.2 System Implementation and Configuration

The system is consisting from the following elements: -

1. Battery: The battery that is uses for the test the lithium ion battery with capacity 600mah and full charger voltage of 3.7V
2. Harvester module (including the power management circuit): Microgen (MPC-00010-00) harvester module is used with the following configuration (the small circles shows the location of the switches during the test

   When:

   - SW 1(A, B) is used to select the suitable power management circuit.
   - SW 2A used to enable and disable the harvester.
   - SW 2B is used to enable and disable the voltage dabbling mode.
   - SW 3A is used to connect and disconnect capacitor bank.
   - SW 3B is used to on/off the LED light, which is used to show that the harvester is working.

Figure 4-4 shows Harvester module (including the power management circuit) configuration

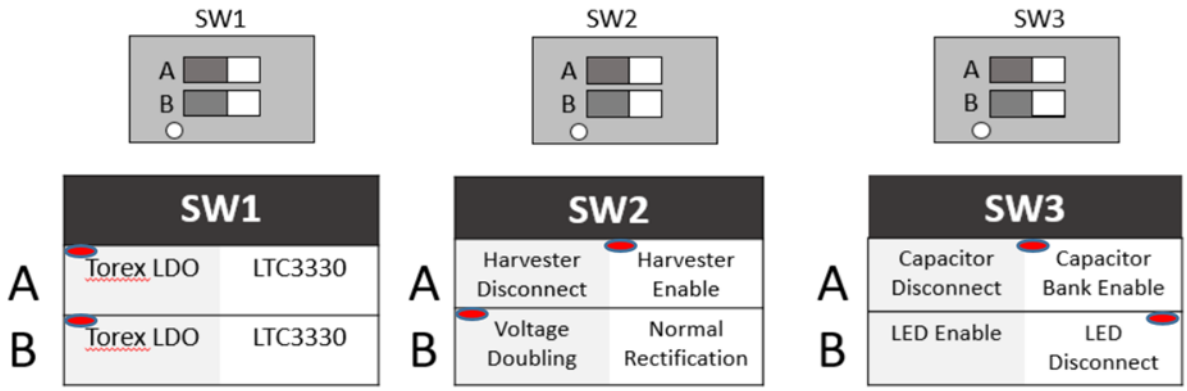

Figure 4-4 harvester configuration

3. Digital multi- meter: It is used to measure the output voltage during the test
4. Iron standard: It is used to fixing the wing to the car
5. UAV wing
6. Wires: It is used to read the output of the harvester inside the wing to the multi meter
7. RC receiver: It is the element that receives the comment from the transmitter and move the flap due to the required position .it is located onboard
8. RC transmitter: It is the control element it is sends the commands to the receiver on the UAV to move the control surfaces and to control the engine throttle.
9. Servomotor (actuator): It is the element that receive the signal from the receiver then translate the signal to flab movement. Figure 4-5 shows micro servo motor

Figure 4-5 micro servo motor

Figure 4-6 illustrates the relation between system elements it is divided to two main part the UAV wing elements and car test rig elements.

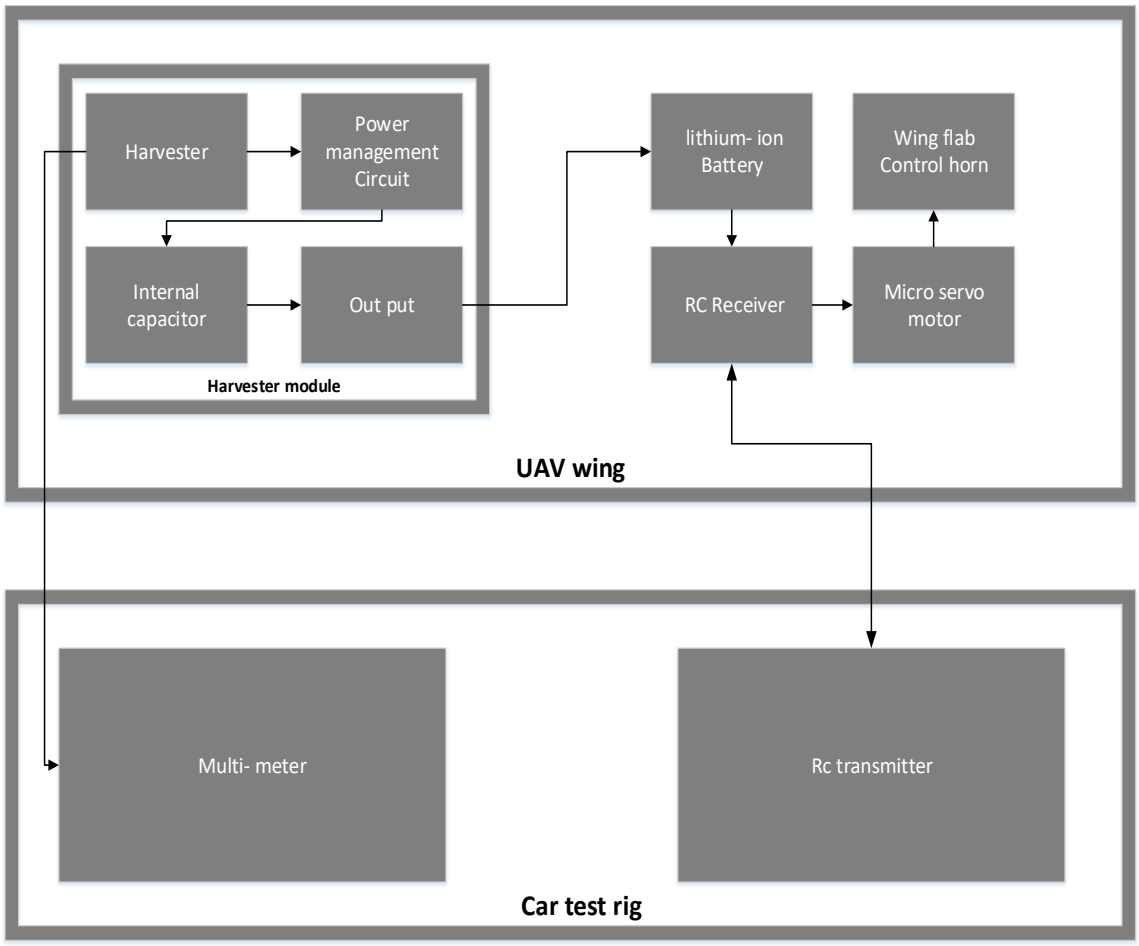

Figure 4-6 system block diagram

Figure 4-7 and Figure 4-8 shows harvesting system element and RC transmitter , receiver and servo motor.

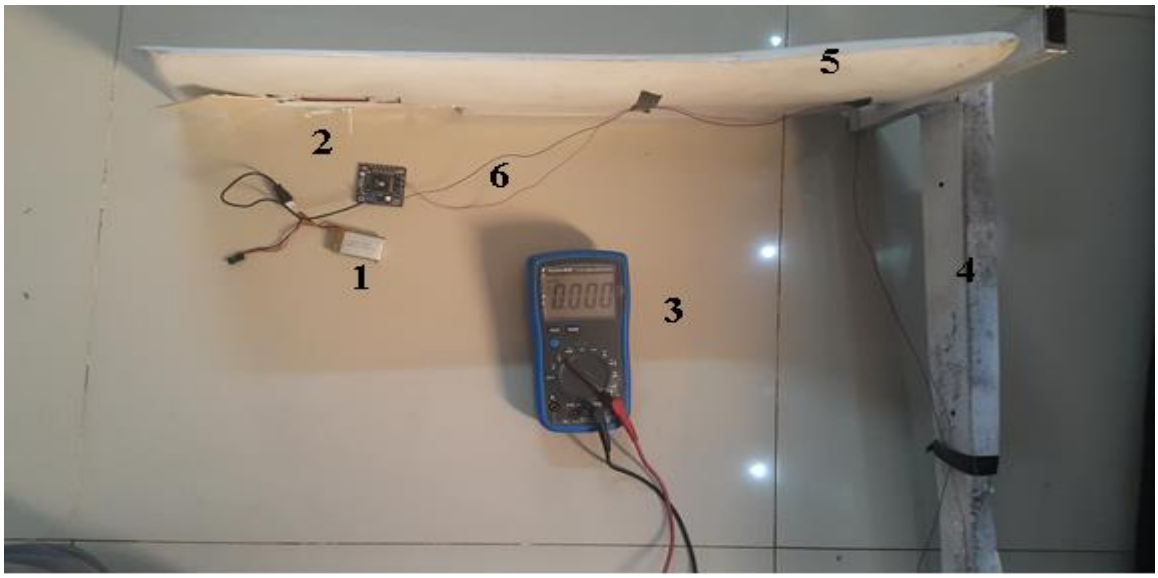

Figure 4-7 harvesting system element

Figure 4-8 RC transmitter, receiver and servo motor

4.3 Car Top Test Rig

When no wind tunnel available for testing, a different testing method was developed byLundström [29] is a rig mounted on the roof of a car. This method was used to test the harvesting system. As illustrated in Figure 4-9 the wing is fixed on the top of the car by iron standard.

Figure 4-9 Car-mounted wing test rig

4.4 Testing

The testing plane is to fix the wing on car rig at its normal position then check that the battery is empty see (Figure 4-10) then install the system inside the wing tip, after that the car will move at the wing charging speed (90km/h) see (Figure 4-11) the multi meter is connected to the harvester to measure the output voltage during the test see fig (Figure 4-12).The test was done on (ALNEEL STREAT) with speed of 90km/h and the output voltage reach 3.719V

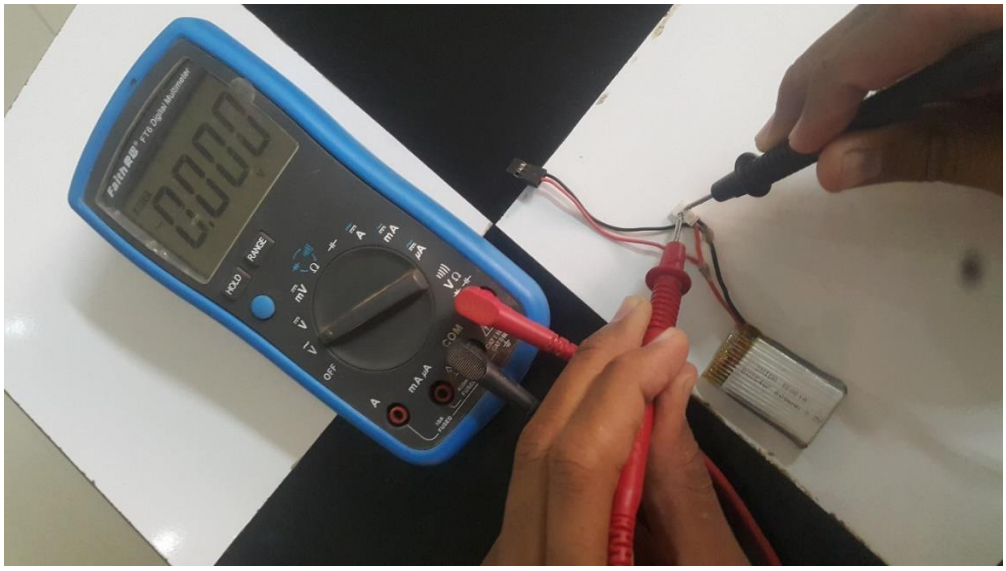

Figure 4-10 battery voltage before testing

Figure 4-11 wing testing on the charging speed

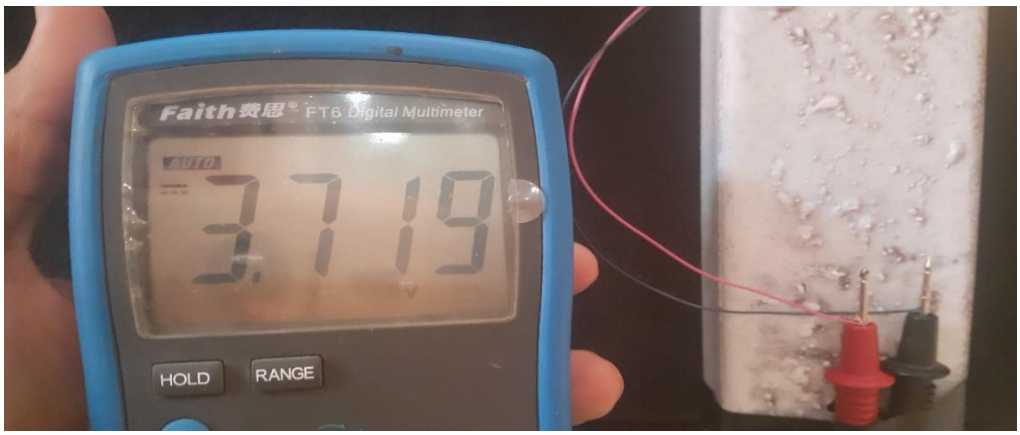

Figure 4-12 output voltage during the test

The test lasting for 20 min for full charge 3.7600mamp lithium- ion battery the harvester output arising at 3.719V. Output power = I* V= 3.719* 0.2=0.7438W

When I= the output current for the Low Power Consumption Voltage Regulator with ON/OFF Switch (XC6215) that is used in the harvester module.

To make comparison to the previous work the most similar example was studied and the comparison result are illustrate in the fig (Figure 4-13) below

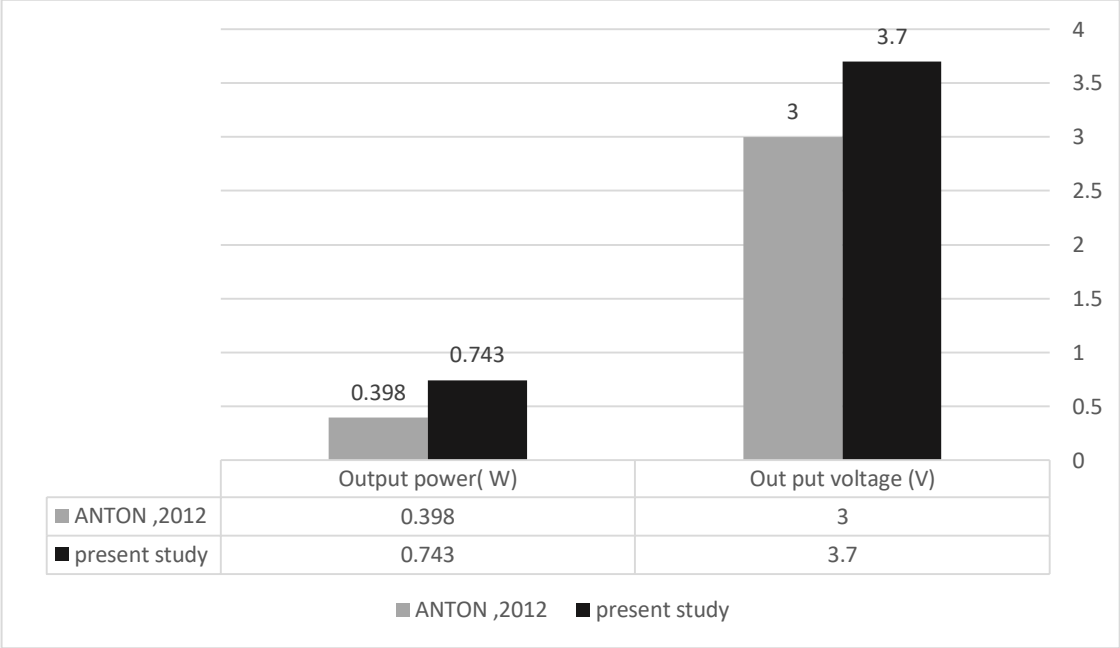

Figure 4-13 Comparison to the previous work

5 CHAPTER FIVE

CONCLUSION AND RECOMMENDATION

5.1 Conclusion

The purpose of this research is to perform a proof of concept study on piezoelectric energy harvesting in UAV applications through car top rig testing of a UAV wing. In addition, to make sure the performance of piezoelectric is reach the maximum amount without making any problems in the UAV structure or the harvesting system. Based on the simulation and testing results we found that there is no relation between the harvested power and the strength of vibration. The piezoelectric material will produce the highest power when it is on resonance mode. By the above methodology it is able to generate the highest power from the piezoelectric material by using the resonance effect on the piezoelectric harvester without any effect or damage on the UAV wing. The output power is 743 mw, which is able to full charge the 600mah battery in 20 min of flight time. the harvested power is able to feed the system of RC receiver and servomotor that is control the movement of the flap in effective way.

5.2 Recommendation

Additional plans for recommended in future work include:

- manufacturing the full model of the mini UAV.
- use the piezoelectric actuator instant of servomotors.
- using the piezoelectric harvesting system as main power source in min UAVS application.

6 REFERENCES

[1] S. R. Anton, "Multifunctional piezoelectric energy harvesting concepts," Virginia Tech, 2011.

[2] IDTechEx, "energy harvesting types " January 2014.

[3] G. W. Taylor and J. R. Burns, "Hydro-piezoelectric power generation from ocean waves," Ferroelectrics, vol. 49, pp. 101-101, 1983.

[4] E. Häsler, L. Stein, and G. Harbauer, "Implantable physiological power supply with PVDF film," Ferroelectrics, vol. 60, pp. 277-282, 1984.

[5] E. Hausler and L. Stein, "Hydromechanical and physiological mechanical-to-electrical power converter with PVDF film," Ferroelectrics, vol. 75, pp. 363-369, 1987.

[6] C. Williams and R. B. Yates, "Analysis of a micro-electric generator for microsystems," sensors and actuators A: Physical, vol. 52, pp. 8-11, 1996.

[7] S. Roundy and P. K. Wright, "A piezoelectric vibration based generator for wireless electronics," Smart Materials and structures, vol. 13, p. 1131, 2004.

[8] N. E. DuToit and B. L. Wardle, "Experimental verification of models for microfabricated piezoelectric vibration energy harvesters," AIAA journal, vol. 45, pp. 1126-1137, 2007.

[9] N. W. Hagood, W. H. Chung, and A. Von Flotow, "Modelling of piezoelectric actuator dynamics for active structural control," Journal of Intelligent Material Systems and Structures, vol. 1, pp. 327-354, 1990.

[10] H. A. Sodano, G. Park, and D. Inman, "Estimation of electric charge output for piezoelectric energy harvesting," Strain, vol. 40, pp. 49-58, 2004.

[11] N. G. Elvin and A. A. Elvin, "A general equivalent circuit model for piezoelectric generators," Journal of Intelligent Material Systems and Structures, vol. 20, pp. 3-9, 2009.

[12] A. Erturk and D. J. Inman, "A distributed parameter electromechanical model for cantilevered piezoelectric energy harvesters," Journal of vibration and acoustics, vol. 130, p. 041002, 2008.

[13] A. Erturk and D. J. Inman, "An experimentally validated bimorph cantilever model for piezoelectric energy harvesting from base excitations," Smart materials and structures, vol. 18, p. 025009, 2009.

[14] H. A. Sodano, D. J. Inman, and G. Park, "Comparison of piezoelectric energy harvesting devices for recharging batteries," Journal of intelligent material systems and structures, vol. 16, pp. 799-807, 2005.

[15] C. Lee, J. Joo, S. Han, J. Lee, and S. Koh, "Poly (vinylidene fluoride) transducers with highly conducting poly (3, 4-ethylenedioxythiophene) electrodes," Synthetic metals, vol. 152, pp. 49-52, 2005.

[16] y. wang, "MRI Compatibility Evaluation of a Piezoelectric Actuator System for a Neural Interventional Robot," ieee 2010.

[17] O. a. G. teams. (2011). https://www.tech.co.

[18] B. Pratihari, "PIEZOELECTRIC CAR " slideshare, Jan 1, 2015.

[19] J. Zhao, and Zheng You, "A shoe-embedded piezoelectric energy harvester for wearable sensors," Sensors 14, no. 7, 2014.

[20] C. De Marqui Jr, Erturk, A., and Inman, D. J., "Piezoaeroelastic modeling and analysis of a generator wing with continuous and segmented electrodes," Journal of Intelligent Material Systems and Structures, 2010.

[21] C. De Marqui Jr, Erturk, A., and Inman, D. J., "An electromechanical finite element model for piezoelectric energy harvester plates," Journal of Sound and Vibration, 2009.

[22] A. a. I. Erturk, D.J, "A distributed parameter electromechanical model for cantilevered piezoelectric energy harvesters," vibration and acoustics, 2008.

[23] A. a. I. Erturk, D. J, "An experimentally validated bimorph cantilever model for piezoelectric energy harvesting from base excitations," Smart Materials and Structures, 2009.

[24] H. Durou, Rossi, C., Brunet, M., Vanhecke, C., Bailly, N., Ardila, G., Ourak, L., Ramond, and S. A., P., and Taberna, "ower harvesting and management from vibrations: A multi-source strategy simulation for aircraft structure health monitoring," SPIE Conference on Smart Structures, Devices, and Systems IV, 2008.

[25] S. Moss, Powlesland, I., Galea, S., and Carman, G, "Vibro-impacting power harvester," 17th SPIE Annual International Symposium on Smart tructures and Materials & Nondestructive Evaluation and Health Monitoring, 2010.

[26] C. Featherston, Holford, K., and Greaves, B, "Harvesting vibration energy for structural health monitoring in aircraft," Key Engineering Materials, 2009.

[27] T. B. Apker, "Simulation of an ornithopter with active flow control and aeroelastic energy harvesting," AIAA Modeling and Simulation Technologies Conference and Exhibit, 2006,.

[28] K. C. Magoteaux, Sanders, B., and Sodano, "Investigation of an energy harvesting small unmanned air vehicle," 15th SPIE Annual International Symposium on Smart Structures and Materials & Nondestructive Evaluation and Health Monitoring, 2008.

[29] D. Lundström, "Aircraft Design Automation and Subscale Testing With Special Reference to Micro Air Vehicles," Linköping University, 2012.

7 APPENDIX A PANEL METHOD PRESSURE OUTPUT

cx	cy	Cz	cp	delta pressure (N/m^2)
0.261536	-0.5443	0.027591	0.292871	1148.053187
0.251956	-0.5443	0.02749	0.262275	1028.117934
0.242386	-0.5443	0.026697	0.201726	790.7645573
0.232838	-0.5443	0.025598	0.141338	554.0447953
0.223313	-0.5443	0.02434	0.082436	323.148664
0.213811	-0.5443	0.023018	0.025279	99.09366883
0.204331	-0.5443	0.021697	-0.03174	-124.4248652
0.19487	-0.5443	0.020441	-0.08874	-347.8486314
0.185426	-0.5443	0.019312	-0.14354	-562.6867109
0.175997	-0.5443	0.018375	-0.19327	-757.6091485
0.166579	-0.5443	0.017703	-0.22651	-887.9007917
0.157167	-0.5443	0.017329	-0.23794	-932.7192518
0.147757	-0.5443	0.017236	-0.23343	-915.0573581
0.138344	-0.5443	0.017379	-0.22394	-877.847238
0.128926	-0.5443	0.017725	-0.2159	-846.3338385
0.119499	-0.5443	0.018277	-0.20918	-819.9736269
0.110059	-0.5443	0.019056	-0.20197	-791.7038546
0.100597	-0.5443	0.020116	-0.19384	-759.8385758
0.093481	-0.5443	0.021115	-0.18928	-741.9865389
0.088715	-0.5443	0.021981	-0.18872	-739.7686257
0.083918	-0.5443	0.023086	-0.18624	-730.0800262
0.080289	-0.5443	0.024157	-0.21978	-861.5412839
0.078567	-0.5443	0.024856	-0.25836	-1012.770439
0.07781	-0.5443	0.025297	-0.21136	-828.5439476
0.076899	-0.5443	0.026438	0.285857	1120.560584

0.076544	-0.5443	0.028544	0.948252	3717.149522
0.077059	-0.5443	0.02995	0.501339	1965.248208
0.077727	-0.5443	0.030608	0.387199	1517.820225
0.079332	-0.5443	0.031748	0.214701	841.6269796
0.082831	-0.5443	0.033614	0.03242	127.0882315
0.087538	-0.5443	0.035623	-0.11105	-435.3106471
0.092276	-0.5443	0.037253	-0.18206	-713.6651724
0.099416	-0.5443	0.0392	-0.24803	-972.2940709
0.108962	-0.5443	0.04132	-0.31017	-1215.856801
0.11853	-0.5443	0.042943	-0.34838	-1365.661407
0.128111	-0.5443	0.044163	-0.37628	-1475.027873
0.1377	-0.5443	0.045024	-0.39828	-1561.258768
0.147295	-0.5443	0.045543	-0.41886	-1641.936754
0.156893	-0.5443	0.045696	-0.43174	-1692.440297
0.166489	-0.5443	0.045442	-0.42285	-1657.584179
0.176079	-0.5443	0.04477	-0.3889	-1524.504391
0.185658	-0.5443	0.043714	-0.33582	-1316.405281
0.195222	-0.5443	0.042338	-0.27486	-1077.452529
0.204768	-0.5443	0.040705	-0.21201	-831.0641164
0.214296	-0.5443	0.038871	-0.15092	-591.6041333
0.223802	-0.5443	0.03688	-0.09032	-354.0413427
0.233285	-0.5443	0.034777	-0.03066	-120.204759
0.242745	-0.5443	0.032618	0.030861	120.9733855
0.252184	-0.5443	0.030468	0.090257	353.8085377
0.261612	-0.5443	0.028401	0.115217	451.6497594
0.261536	-0.47323	0.022622	0.325468	1275.836152
0.251956	-0.47323	0.02252	0.295568	1158.627996
0.242386	-0.47323	0.021727	0.234981	921.1265639
0.232838	-0.47323	0.020629	0.171742	673.2282232

0.223313	-0.47323	0.01937	0.107642	421.9573036
0.213811	-0.47323	0.018048	0.043207	169.3721434
0.204331	-0.47323	0.016727	-0.02271	-89.03282585
0.19487	-0.47323	0.015471	-0.08963	-351.3489594
0.185426	-0.47323	0.014342	-0.1547	-606.4156633
0.175997	-0.47323	0.013405	-0.21415	-839.4534846
0.166579	-0.47323	0.012733	-0.25541	-1001.203363
0.157167	-0.47323	0.012359	-0.27232	-1067.476484
0.147757	-0.47323	0.012266	-0.27075	-1061.347641
0.138344	-0.47323	0.012409	-0.26236	-1028.437538
0.128926	-0.47323	0.012756	-0.25419	-996.4197293
0.119499	-0.47323	0.013307	-0.24625	-965.3099489
0.110059	-0.47323	0.014086	-0.23645	-926.8790497
0.100597	-0.47323	0.015146	-0.22351	-876.1775069
0.093481	-0.47323	0.016146	-0.21256	-833.2515301
0.088715	-0.47323	0.017012	-0.20498	-803.5211918
0.083918	-0.47323	0.018116	-0.19134	-750.058858
0.080289	-0.47323	0.019187	-0.21239	-832.5614093
0.078567	-0.47323	0.019886	-0.2435	-954.5040221
0.07781	-0.47323	0.020327	-0.1945	-762.4553654
0.076899	-0.47323	0.021468	0.301774	1182.952332
0.076544	-0.47323	0.023574	0.943611	3698.955936
0.077059	-0.47323	0.024981	0.488263	1913.99273
0.077727	-0.47323	0.025638	0.372921	1461.84905
0.079332	-0.47323	0.026779	0.194013	760.5294738
0.082831	-0.47323	0.028644	-0.00286	-11.22533953
0.087538	-0.47323	0.030653	-0.16326	-639.986125
0.092276	-0.47323	0.032283	-0.24705	-968.4518341
0.099416	-0.47323	0.03423	-0.328	-1285.761698

0.108962	-0.47323	0.03635	-0.40604	-1591.668436
0.11853	-0.47323	0.037973	-0.45696	-1791.289471
0.128111	-0.47323	0.039194	-0.49519	-1941.154284
0.1377	-0.47323	0.040054	-0.52554	-2060.111788
0.147295	-0.47323	0.040573	-0.55284	-2167.116273
0.156893	-0.47323	0.040727	-0.56982	-2233.711273
0.166489	-0.47323	0.040472	-0.56051	-2197.203399
0.176079	-0.47323	0.0398	-0.52112	-2042.77314
0.185658	-0.47323	0.038744	-0.45851	-1797.347888
0.195222	-0.47323	0.037368	-0.38557	-1511.424512
0.204768	-0.47323	0.035735	-0.30916	-1211.902129
0.214296	-0.47323	0.033901	-0.23305	-913.5729437
0.223802	-0.47323	0.03191	-0.15532	-608.8502895
0.233285	-0.47323	0.029808	-0.07578	-297.0761409
0.242745	-0.47323	0.027648	0.007797	30.56603458
0.252184	-0.47323	0.025499	0.088647	347.4977514
0.261612	-0.47323	0.023431	0.123503	484.1315277
0.261536	-0.35823	0.01458	0.328309	1286.971717
0.251956	-0.35823	0.014479	0.298468	1169.994799
0.242386	-0.35823	0.013686	0.238167	933.6138277
0.232838	-0.35823	0.012587	0.17496	685.8434352
0.223313	-0.35823	0.011329	0.110592	433.521373
0.213811	-0.35823	0.010007	0.045619	178.827116
0.204331	-0.35823	0.008686	-0.02102	-82.40571954
0.19487	-0.35823	0.00743	-0.0888	-348.0955845
0.185426	-0.35823	0.006301	-0.15479	-606.7686181
0.175997	-0.35823	0.005363	-0.21504	-842.9620359
0.166579	-0.35823	0.004692	-0.2569	-1007.033025
0.157167	-0.35823	0.004318	-0.27418	-1074.803202

0.147757	-0.35823	0.004225	-0.27256	-1068.435381
0.138344	-0.35823	0.004367	-0.26337	-1032.421819
0.128926	-0.35823	0.004714	-0.2538	-994.8847361
0.119499	-0.35823	0.005266	-0.24389	-956.0333399
0.110059	-0.35823	0.006045	-0.23128	-906.606229
0.100597	-0.35823	0.007105	-0.21424	-839.8054056
0.093481	-0.35823	0.008104	-0.19876	-779.1216489
0.088715	-0.35823	0.00897	-0.18673	-731.9642416
0.083918	-0.35823	0.010075	-0.16552	-648.8448432
0.080289	-0.35823	0.011146	-0.17445	-683.8294064
0.078567	-0.35823	0.011845	-0.19366	-759.1412952
0.07781	-0.35823	0.012286	-0.13733	-538.329577
0.076899	-0.35823	0.013427	0.360945	1414.904785
0.076544	-0.35823	0.015533	0.922594	3616.568997
0.077059	-0.35823	0.016939	0.437693	1715.757675
0.077727	-0.35823	0.017597	0.323595	1268.491047
0.079332	-0.35823	0.018737	0.146432	574.013226
0.082831	-0.35823	0.020603	-0.04718	-184.9510731
0.087538	-0.35823	0.022612	-0.20668	-810.2017941
0.092276	-0.35823	0.024242	-0.2906	-1139.170786
0.099416	-0.35823	0.026189	-0.37311	-1462.597226
0.108962	-0.35823	0.028309	-0.45388	-1779.198956
0.11853	-0.35823	0.029932	-0.50748	-1989.320295
0.128111	-0.35823	0.031152	-0.54822	-2149.012538
0.1377	-0.35823	0.032013	-0.58059	-2275.896594
0.147295	-0.35823	0.032531	-0.60921	-2388.109096
0.156893	-0.35823	0.032685	-0.62639	-2455.449951
0.166489	-0.35823	0.032431	-0.61557	-2413.020437
0.176079	-0.35823	0.031759	-0.57299	-2246.13113

0.185658	-0.35823	0.030703	-0.50574	-1982.502247
0.195222	-0.35823	0.029327	-0.42723	-1674.72341
0.204768	-0.35823	0.027694	-0.34484	-1351.753727
0.214296	-0.35823	0.02586	-0.26255	-1029.187259
0.223802	-0.35823	0.023869	-0.1786	-700.1139597
0.233285	-0.35823	0.021766	-0.09303	-364.6797851
0.242745	-0.35823	0.019607	-0.00378	-14.80957985
0.252184	-0.35823	0.017457	0.082195	322.2050441
0.261612	-0.35823	0.01539	0.119393	468.0203608
0.261536	-0.24323	0.006539	0.328942	1289.454205
0.251956	-0.24323	0.006437	0.299179	1172.780738
0.242386	-0.24323	0.005645	0.239142	937.4366202
0.232838	-0.24323	0.004546	0.176174	690.6034357
0.223313	-0.24323	0.003288	0.11195	438.8455623
0.213811	-0.24323	0.001966	0.047058	184.4673901
0.204331	-0.24323	0.000645	-0.01954	-76.61074889
0.19487	-0.24323	-0.00061	-0.08733	-342.3427486
0.185426	-0.24323	-0.00174	-0.15337	-601.1949603
0.175997	-0.24323	-0.00268	-0.21373	-837.8322325
0.166579	-0.24323	-0.00335	-0.25574	-1002.515247
0.157167	-0.24323	-0.00372	-0.27308	-1070.49137
0.147757	-0.24323	-0.00382	-0.27151	-1064.308284
0.138344	-0.24323	-0.00367	-0.26257	-1029.262523
0.128926	-0.24323	-0.00333	-0.25309	-992.1065445
0.119499	-0.24323	-0.00278	-0.24285	-951.9550099
0.110059	-0.24323	-0.002	-0.22942	-899.3459322
0.100597	-0.24323	-0.00094	-0.21071	-825.9945592
0.093481	-0.24323	6.32E-05	-0.19304	-756.7126523
0.088715	-0.24323	0.000929	-0.17833	-699.0451077

0.083918	-0.24323	0.002033	-0.15237	-597.2921507
0.080289	-0.24323	0.003104	-0.1535	-601.7184154
0.078567	-0.24323	0.003804	-0.16485	-646.224946
0.07781	-0.24323	0.004245	-0.10331	-404.9891009
0.076899	-0.24323	0.005385	0.397771	1559.262506
0.076544	-0.24323	0.007491	0.905907	3551.156024
0.077059	-0.24323	0.008898	0.399753	1567.030936
0.077727	-0.24323	0.009556	0.286439	1122.842264
0.079332	-0.24323	0.010696	0.110463	433.0142326
0.082831	-0.24323	0.012562	-0.08065	-316.131978
0.087538	-0.24323	0.014571	-0.23873	-935.8402183
0.092276	-0.24323	0.016201	-0.32191	-1261.887696
0.099416	-0.24323	0.018147	-0.4038	-1582.915204
0.108962	-0.24323	0.020268	-0.48407	-1897.567754
0.11853	-0.24323	0.021891	-0.5371	-2105.450515
0.128111	-0.24323	0.023111	-0.57705	-2262.041788
0.1377	-0.24323	0.023971	-0.60836	-2384.757706
0.147295	-0.24323	0.02449	-0.63581	-2492.357876
0.156893	-0.24323	0.024644	-0.65164	-2554.41398
0.166489	-0.24323	0.024389	-0.63901	-2504.92848
0.176079	-0.24323	0.023718	-0.59404	-2328.637971
0.185658	-0.24323	0.022662	-0.52413	-2054.571756
0.195222	-0.24323	0.021285	-0.44298	-1736.479037
0.204768	-0.24323	0.019653	-0.35802	-1403.447793
0.214296	-0.24323	0.017818	-0.27335	-1071.531175
0.223802	-0.24323	0.015827	-0.1872	-733.8299523
0.233285	-0.24323	0.013725	-0.0996	-390.4373399
0.242745	-0.24323	0.011566	-0.00855	-33.51448972
0.252184	-0.24323	0.009416	0.079076	309.9770163

0.261612	-0.24323	0.007349	0.117078	458.9462497
0.261536	-0.17216	0.001569	0.331746	1300.443834
0.251956	-0.17216	0.001468	0.302185	1184.563338
0.242386	-0.17216	0.000675	0.24259	950.9515465
0.232838	-0.17216	-0.00042	0.18025	706.5783948
0.223313	-0.17216	-0.00168	0.116875	458.1507878
0.213811	-0.17216	-0.003	0.052907	207.3951935
0.204331	-0.17216	-0.00432	-0.01288	-50.47569996
0.19487	-0.17216	-0.00558	-0.08015	-314.1879804
0.185426	-0.17216	-0.00671	-0.14615	-572.925681
0.175997	-0.17216	-0.00765	-0.20713	-811.9360143
0.166579	-0.17216	-0.00832	-0.25065	-982.5533758
0.157167	-0.17216	-0.00869	-0.27029	-1059.530156
0.147757	-0.17216	-0.00879	-0.27167	-1064.927781
0.138344	-0.17216	-0.00864	-0.26624	-1043.664215
0.128926	-0.17216	-0.0083	-0.2609	-1022.744797
0.119499	-0.17216	-0.00775	-0.2556	-1001.947852
0.110059	-0.17216	-0.00697	-0.24796	-972.0076027
0.100597	-0.17216	-0.00591	-0.23562	-923.613562
0.093481	-0.17216	-0.00491	-0.22241	-871.8358323
0.088715	-0.17216	-0.00404	-0.21001	-823.2519774
0.083918	-0.17216	-0.00294	-0.18453	-723.3578383
0.080289	-0.17216	-0.00187	-0.18467	-723.913948
0.078567	-0.17216	-0.00117	-0.19444	-762.1931897
0.07781	-0.17216	-0.00072	-0.13002	-509.6951612
0.076899	-0.17216	0.000416	0.386631	1515.594221
0.076544	-0.17216	0.002522	0.901637	3534.415527
0.077059	-0.17216	0.003928	0.37788	1481.290604
0.077727	-0.17216	0.004586	0.259754	1018.235448

0.079332	-0.17216	0.005726	0.077035	301.9780879
0.082831	-0.17216	0.007592	-0.12218	-478.9478134
0.087538	-0.17216	0.009601	-0.28656	-1123.300863
0.092276	-0.17216	0.011231	-0.37195	-1458.02489
0.099416	-0.17216	0.013178	-0.45365	-1778.309867
0.108962	-0.17216	0.015298	-0.53067	-2080.212386
0.11853	-0.17216	0.016921	-0.57879	-2268.873233
0.128111	-0.17216	0.018141	-0.61332	-2404.229548
0.1377	-0.17216	0.019002	-0.63911	-2505.325906
0.147295	-0.17216	0.01952	-0.66113	-2591.627902
0.156893	-0.17216	0.019674	-0.67154	-2632.422332
0.166489	-0.17216	0.01942	-0.65341	-2561.354398
0.176079	-0.17216	0.018748	-0.60318	-2364.459491
0.185658	-0.17216	0.017692	-0.52877	-2072.791173
0.195222	-0.17216	0.016316	-0.44407	-1740.754543
0.204768	-0.17216	0.014683	-0.35654	-1397.635544
0.214296	-0.17216	0.012849	-0.27016	-1059.033809
0.223802	-0.17216	0.010858	-0.18307	-717.6449429
0.233285	-0.17216	0.008755	-0.0951	-372.7733942
0.242745	-0.17216	0.006596	-0.00404	-15.82878498
0.252184	-0.17216	0.004446	0.083181	326.0700621
0.261612	-0.17216	0.002379	0.120858	473.7621512
0.261295	-0.13346	0.000206	0.331793	1300.626924
0.251235	-0.13346	9.88E-05	0.302216	1184.687149
0.241186	-0.13346	-0.00073	0.242787	951.7267315
0.231159	-0.13346	-0.00189	0.180828	708.8475302
0.221157	-0.13346	-0.00321	0.117953	462.3766161
0.211178	-0.13346	-0.0046	0.054512	213.6869848
0.201223	-0.13346	-0.00598	-0.01072	-42.00371977

0.191287	-0.13346	-0.0073	-0.07739	-303.3661146
0.18137	-0.13346	-0.00849	-0.14276	-559.6195915
0.171468	-0.13346	-0.00947	-0.20308	-796.0577396
0.161577	-0.13346	-0.01018	-0.24598	-964.2268351
0.151694	-0.13346	-0.01057	-0.26527	-1039.871931
0.141812	-0.13346	-0.01067	-0.2665	-1044.697352
0.131927	-0.13346	-0.01052	-0.26087	-1022.593622
0.122037	-0.13346	-0.01016	-0.25506	-999.8532941
0.112137	-0.13346	-0.00958	-0.24886	-975.5359405
0.102223	-0.13346	-0.00876	-0.23949	-938.8015839
0.092287	-0.13346	-0.00765	-0.22365	-876.7164822
0.084814	-0.13346	-0.0066	-0.20586	-806.9782677
0.079809	-0.13346	-0.00569	-0.18904	-741.0201567
0.074772	-0.13346	-0.00453	-0.1588	-622.4818767
0.07096	-0.13346	-0.0034	-0.15149	-593.8570096
0.069153	-0.13346	-0.00267	-0.15341	-601.3589327
0.068357	-0.13346	-0.0022	-0.10201	-399.8700898
0.067401	-0.13346	-0.00101	0.312375	1224.511
0.067028	-0.13346	0.001206	0.731298	2866.688717
0.067569	-0.13346	0.002683	0.349119	1368.547078
0.068271	-0.13346	0.003373	0.255771	1002.621054
0.069956	-0.13346	0.004571	0.098293	385.3072771
0.07363	-0.13346	0.00653	-0.08509	-333.5551966
0.078574	-0.13346	0.00864	-0.24295	-952.3549617
0.083549	-0.13346	0.010352	-0.3304	-1295.165612
0.091047	-0.13346	0.012396	-0.41835	-1639.93789
0.101072	-0.13346	0.014622	-0.50258	-1970.120061
0.111119	-0.13346	0.016327	-0.55612	-2179.979903
0.12118	-0.13346	0.017609	-0.59464	-2330.990787

0.131251	-0.13346	0.018512	-0.62345	-2443.923301
0.141327	-0.13346	0.019057	-0.64781	-2539.432333
0.151406	-0.13346	0.019218	-0.66026	-2588.23655
0.161483	-0.13346	0.018951	-0.64432	-2525.717966
0.171554	-0.13346	0.018245	-0.59637	-2337.781048
0.181613	-0.13346	0.017137	-0.52403	-2054.194015
0.191657	-0.13346	0.015691	-0.44113	-1729.238615
0.201682	-0.13346	0.013977	-0.35514	-1392.166865
0.211687	-0.13346	0.01205	-0.27008	-1058.716245
0.22167	-0.13346	0.00996	-0.184	-721.2712603
0.231628	-0.13346	0.007752	-0.09669	-379.0321453
0.241563	-0.13346	0.005484	-0.00585	-22.92873156
0.251475	-0.13346	0.003227	0.081638	320.0203387
0.261375	-0.13346	0.001056	0.119557	468.6636394
0.260575	-0.07626	0.000235	0.327492	1283.770169
0.249074	-0.07626	0.000113	0.29755	1166.396876
0.237585	-0.07626	-0.00084	0.237323	930.3051059
0.226122	-0.07626	-0.00216	0.174422	683.7355302
0.214687	-0.07626	-0.00367	0.110636	433.6945951
0.203279	-0.07626	-0.00526	0.046512	182.326874
0.191898	-0.07626	-0.00684	-0.0189	-74.07328231
0.180539	-0.07626	-0.00835	-0.08494	-332.9581447
0.1692	-0.07626	-0.00971	-0.14868	-582.8061425
0.157881	-0.07626	-0.01083	-0.20633	-808.7962608
0.146573	-0.07626	-0.01164	-0.24552	-962.4321944
0.135274	-0.07626	-0.01209	-0.26031	-1020.428452
0.123976	-0.07626	-0.0122	-0.25661	-1005.907674
0.112676	-0.07626	-0.01203	-0.24561	-962.7893856
0.101368	-0.07626	-0.01161	-0.23407	-917.5527607

0.090051	-0.07626	-0.01095	-0.22203	-870.3733257
0.078717	-0.07626	-0.01001	-0.20769	-814.129272
0.067357	-0.07626	-0.00874	-0.18985	-744.2075978
0.058814	-0.07626	-0.00754	-0.17495	-685.8024811
0.053092	-0.07626	-0.0065	-0.16383	-642.2244531
0.047334	-0.07626	-0.00517	-0.14352	-562.6164794
0.042976	-0.07626	-0.00389	-0.14776	-579.2071584
0.04091	-0.07626	-0.00305	-0.15879	-622.4423147
0.04	-0.07626	-0.00252	-0.11412	-447.3539469
0.038907	-0.07626	-0.00115	0.287533	1127.130279
0.03848	-0.07626	0.001378	0.744691	2919.189153
0.039099	-0.07626	0.003067	0.391996	1536.625628
0.039901	-0.07626	0.003857	0.301727	1182.770663
0.041828	-0.07626	0.005226	0.149273	585.1520966
0.046028	-0.07626	0.007466	-0.02608	-102.2392455
0.05168	-0.07626	0.009878	-0.17295	-677.9543369
0.057368	-0.07626	0.011835	-0.25204	-987.9807426
0.06594	-0.07626	0.014171	-0.33259	-1303.735687
0.0774	-0.07626	0.016717	-0.41473	-1625.75198
0.088887	-0.07626	0.018666	-0.4723	-1851.398594
0.100389	-0.07626	0.020131	-0.51798	-2030.496883
0.111902	-0.07626	0.021163	-0.55545	-2177.374495
0.123422	-0.07626	0.021786	-0.58895	-2308.670402
0.134945	-0.07626	0.021971	-0.61085	-2394.533645
0.146466	-0.07626	0.021666	-0.60483	-2370.942548
0.157979	-0.07626	0.020859	-0.56669	-2221.410029
0.169479	-0.07626	0.019591	-0.50318	-1972.467099
0.180961	-0.07626	0.017939	-0.42763	-1676.313278
0.192422	-0.07626	0.015979	-0.34724	-1361.16746

0.203861	-0.07626	0.013777	-0.26615	-1043.314783
0.215273	-0.07626	0.011386	-0.18281	-716.632244
0.226658	-0.07626	0.008862	-0.09741	-381.829914
0.238016	-0.07626	0.00627	-0.00789	-30.93899012
0.249347	-0.07626	0.003689	0.078662	308.3548373
0.260666	-0.07626	0.001207	0.116209	455.540806
0.259855	-0.01907	0.000264	0.321354	1259.707859
0.246912	-0.01907	0.000127	0.29058	1139.072143
0.233984	-0.01907	-0.00094	0.228576	896.0187459
0.221085	-0.01907	-0.00243	0.163803	642.1064588
0.208217	-0.01907	-0.00413	0.09834	385.4933461
0.19538	-0.01907	-0.00591	0.033203	130.1539636
0.182572	-0.01907	-0.0077	-0.03227	-126.483001
0.16979	-0.01907	-0.0094	-0.09725	-381.2250908
0.157031	-0.01907	-0.01092	-0.15852	-621.3980908
0.144293	-0.01907	-0.01219	-0.21216	-831.6788002
0.131569	-0.01907	-0.0131	-0.24602	-964.4058829
0.118854	-0.01907	-0.0136	-0.25456	-997.8695522
0.106141	-0.01907	-0.01373	-0.24436	-957.9068225
0.093424	-0.01907	-0.01353	-0.22711	-890.2735311
0.0807	-0.01907	-0.01306	-0.20941	-820.869548
0.067965	-0.01907	-0.01232	-0.19095	-748.5166339
0.055211	-0.01907	-0.01127	-0.16938	-663.9646994
0.042428	-0.01907	-0.00984	-0.14313	-561.0591613
0.032814	-0.01907	-0.00848	-0.12116	-474.9411345
0.026375	-0.01907	-0.00731	-0.10573	-414.4437644
0.019895	-0.01907	-0.00582	-0.08305	-325.5507564
0.014992	-0.01907	-0.00438	-0.08746	-342.8485249
0.012666	-0.01907	-0.00343	-0.10085	-395.3195551

0.011643	-0.01907	-0.00284	-0.06206	-243.2874831
0.010413	-0.01907	-0.00129	0.308226	1208.245251
0.009933	-0.01907	0.001551	0.762619	2989.468037
0.010629	-0.01907	0.003451	0.449028	1760.188888
0.011531	-0.01907	0.00434	0.368723	1445.393363
0.0137	-0.01907	0.005881	0.2287	896.5027828
0.018426	-0.01907	0.008401	0.065573	257.0466847
0.024786	-0.01907	0.011115	-0.07414	-290.623032
0.031186	-0.01907	0.013317	-0.15244	-597.5571631
0.040833	-0.01907	0.015947	-0.236	-925.106833
0.053729	-0.01907	0.018812	-0.32475	-1273.002916
0.066655	-0.01907	0.021005	-0.39018	-1529.513891
0.079599	-0.01907	0.022653	-0.4444	-1742.060469
0.092554	-0.01907	0.023815	-0.49107	-1925.000442
0.105517	-0.01907	0.024516	-0.53442	-2094.94386
0.118484	-0.01907	0.024724	-0.56715	-2223.232057
0.131448	-0.01907	0.02438	-0.5725	-2244.215296
0.144403	-0.01907	0.023472	-0.54523	-2137.32
0.157345	-0.01907	0.022046	-0.49111	-1925.136486
0.170265	-0.01907	0.020187	-0.4226	-1656.599949
0.183163	-0.01907	0.017981	-0.34692	-1359.918089
0.196035	-0.01907	0.015503	-0.26852	-1052.592203
0.208877	-0.01907	0.012813	-0.18623	-730.0204263
0.221689	-0.01907	0.009973	-0.10091	-395.5620076
0.234469	-0.01907	0.007055	-0.0113	-44.29814777
0.24722	-0.01907	0.004151	0.075098	294.385927
0.259957	-0.01907	0.001358	0.112474	440.8997758

Where:

Cx is the center of x vector on each panel.

Cy is the center of Y vector on each panel.

Cz is the center of Z vector on each panel.

Cp is the center of pressure on each panel.

Delta pressure: is the average of pressure of each panel. Equal (0.5 *air density *(air velocity) ^2)*cp)

8 APPENDIX B MODE SHAPES

Error! Reference source not found. to Figure 8 Shows the mode shapes from mode 1 to mode 10 respectively

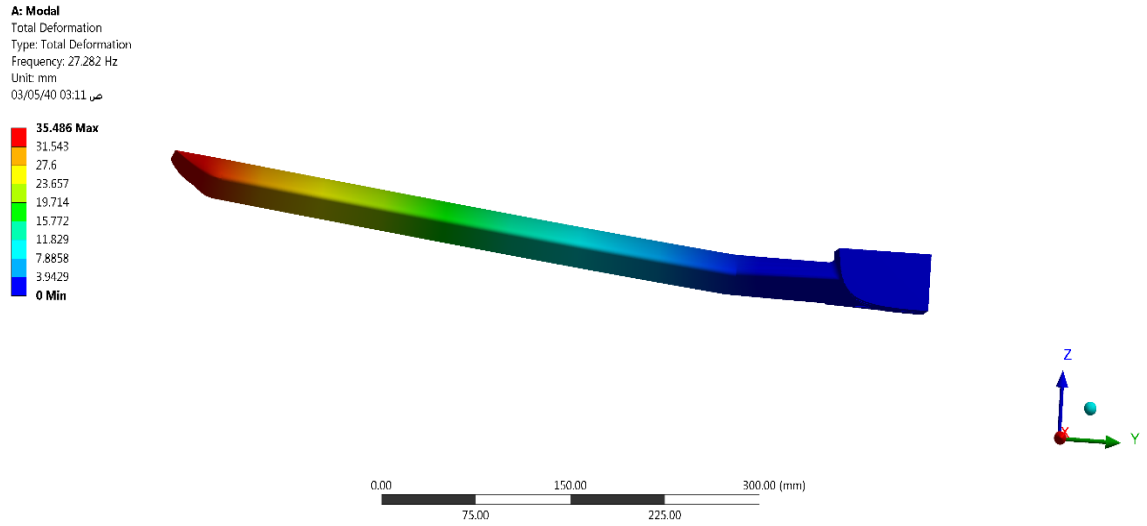

Figure 1: Mode Shape for Mode 1

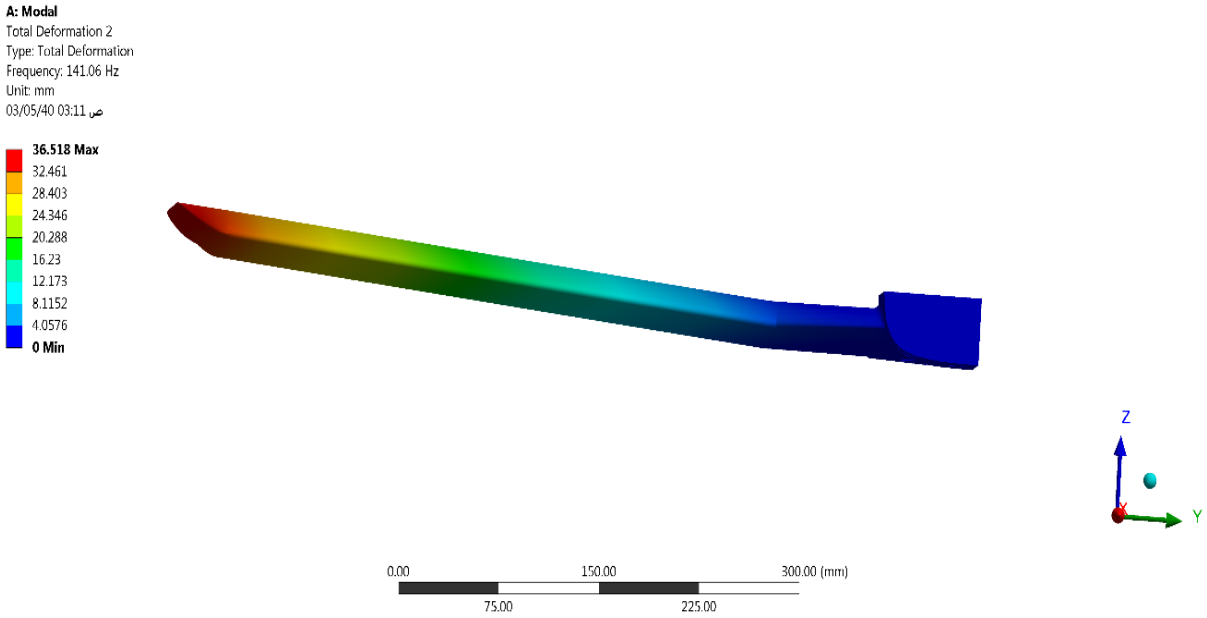

Figure 2: Mode Shape for Mode 2

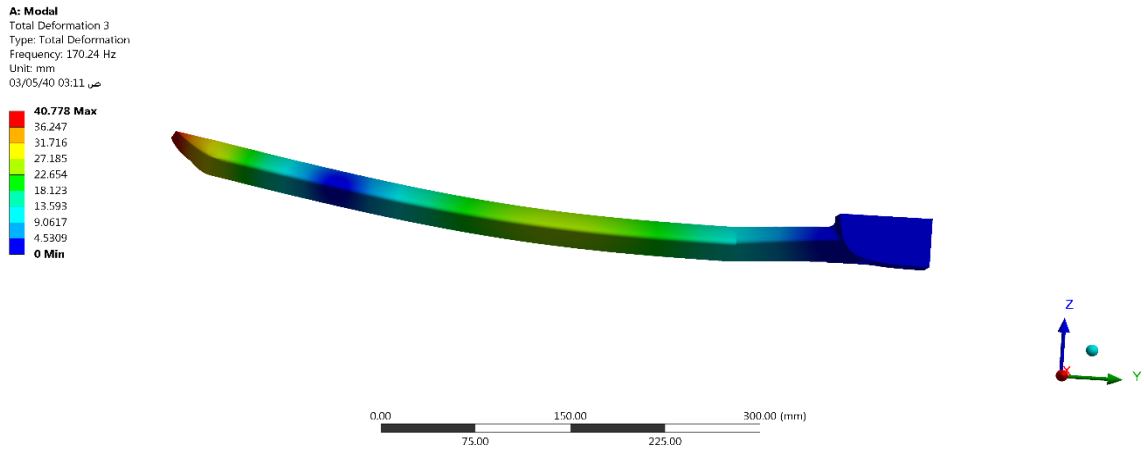

Figure 1:Mode Shape for Mode 3

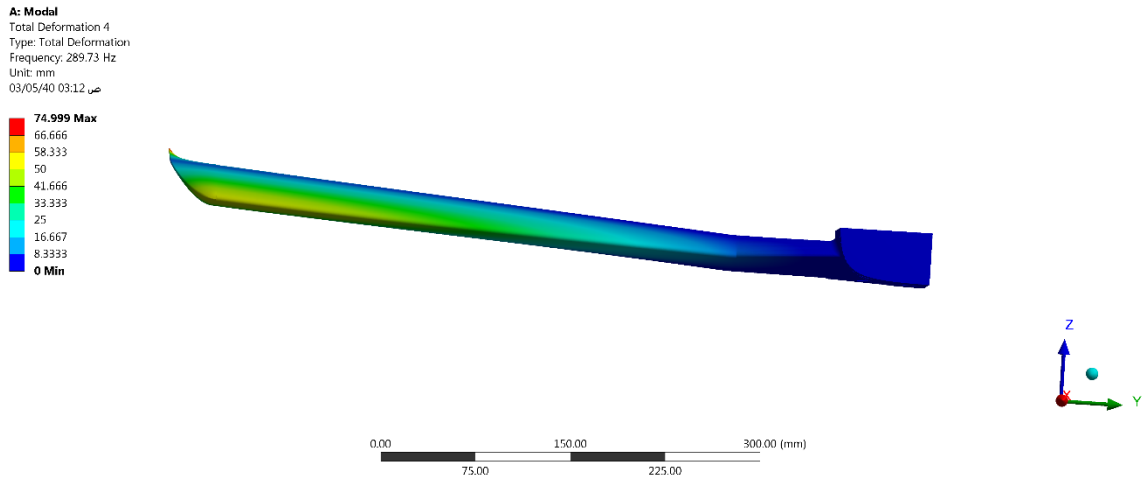

Figure 2:Mode Shape for Mode 4

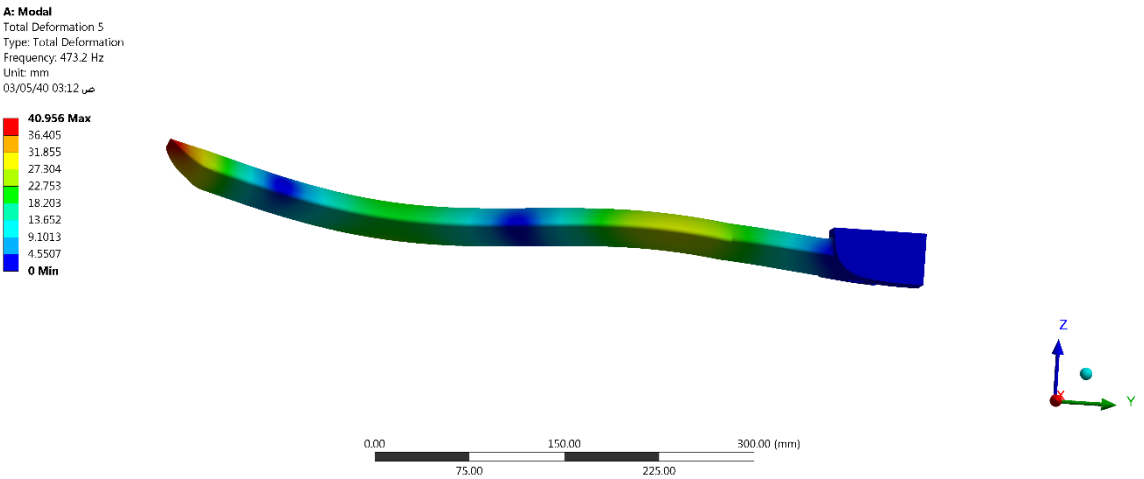

Figure 3:Mode Shape for Mode 5

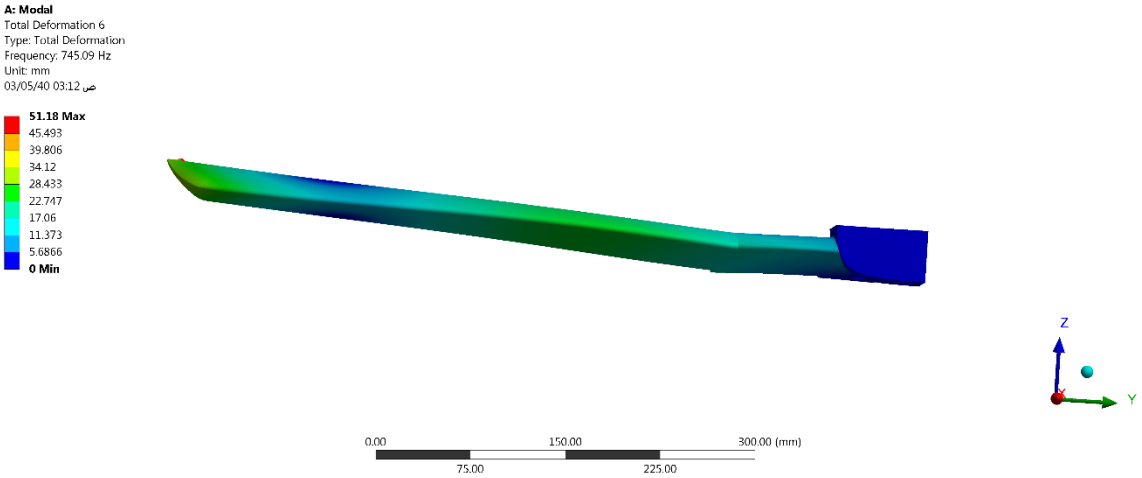

Figure 4: Mode Shape for Mode 6

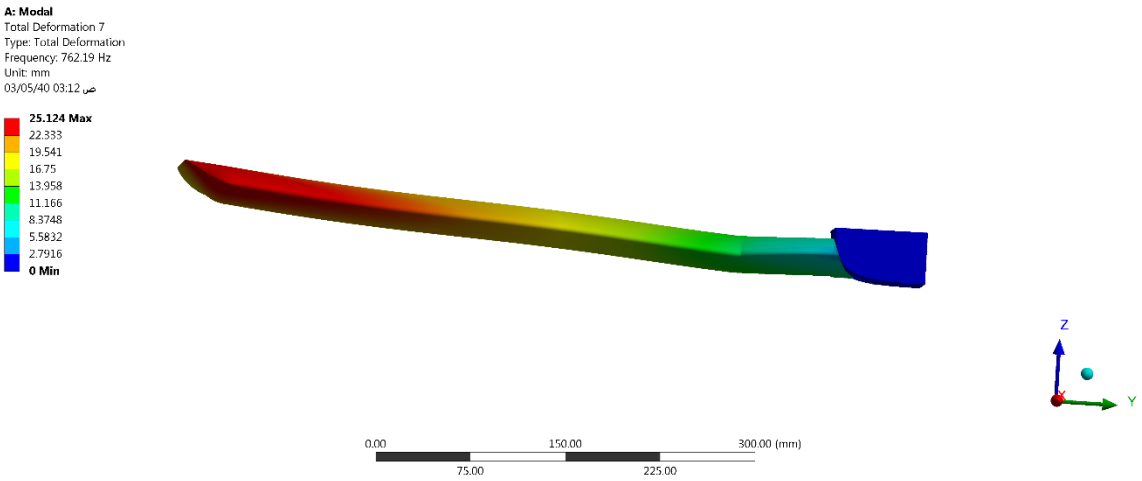

Figure 5: Mode Shape for Mode 7

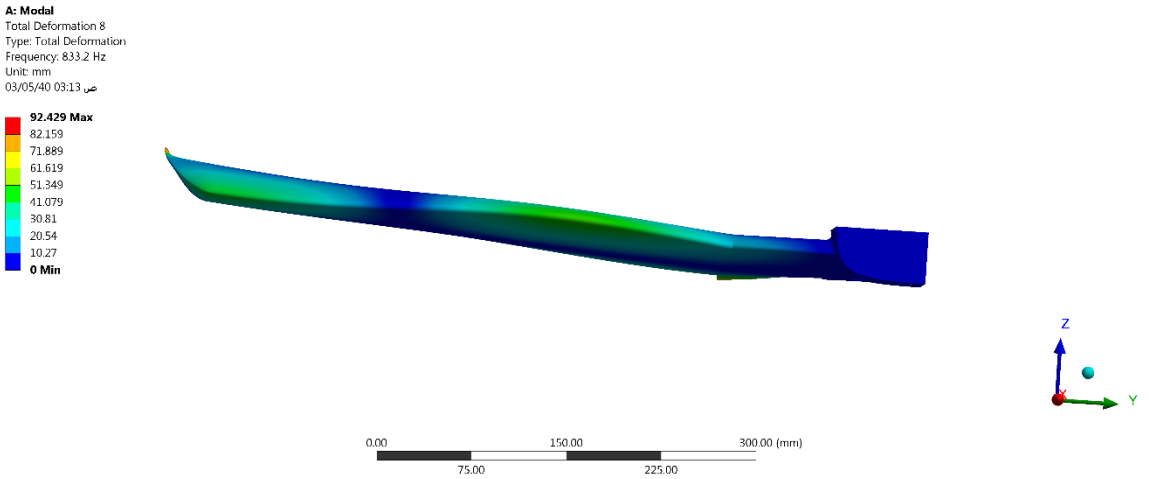

Figure 6: Mode Shape for Mode 8

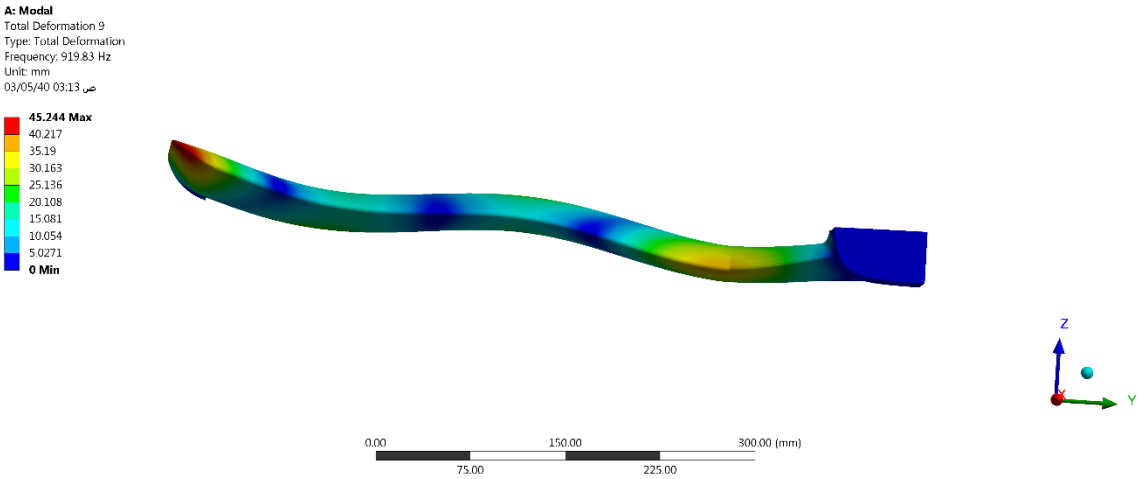

Figure 7: Mode Shape for Mode 9

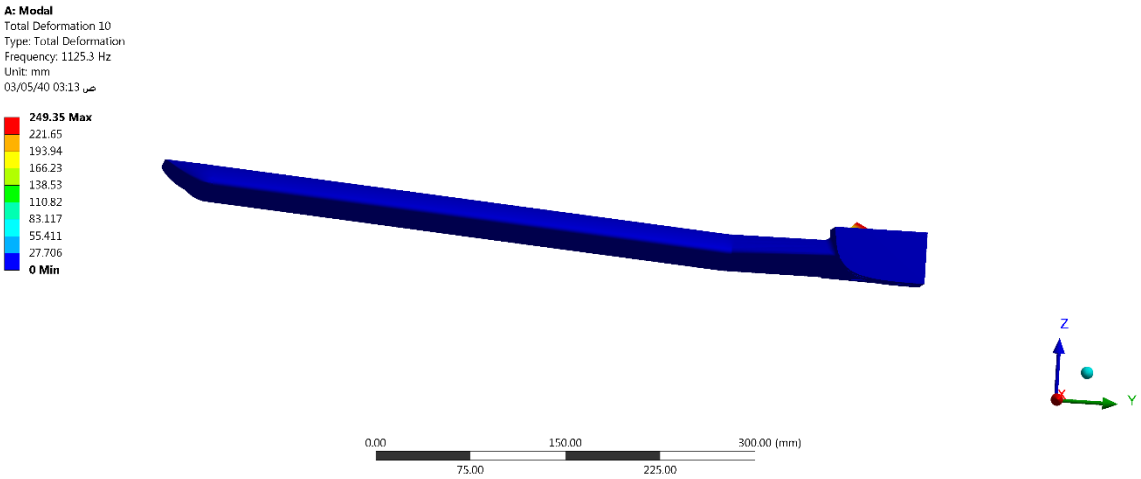

Figure 8: Mode Shape for Mode 10